Sonochemical and Sonoelectrochemical Production of Hydrogen-An Overview

Md Hujjatul Islam, Odne S. Burheim and Bruno G. Pollet*

Department of Energy and Process Engineering,
Faculty of Engineering,
Norwegian University of Science and Technology (NTNU),
NO-7491 Trondheim, Norway
*bruno.g.pollet@ntnu.no

Abstract

Reserves of fossil fuel such as coal, oil and natural gas on earth are finite. Also, the continuous use and burning of these fossil resources in industrial, domestic and transport sectors results in the extremely high emission of greenhouse gases into the atmosphere. Therefore, it is necessary to explore pollution free and more efficient energy sources in order to replace depleting fossil fuels. The use of hydrogen as an alternative fuel source is particularly attractive due to its very high specific energy compared to other conventional fuels. Hydrogen can be produced through various process technologies such as thermal, electrolytic and photolytic processes. Thermal processes include gas reforming, renewable liquid and biooil processing, biomass and coal gasification; however, these processes release a huge amount of greenhouse gases. Production of hydrogen from water using ultrasound could be a promising technique to produce clean hydrogen. Also, using ultrasound in water electrolysis could be a promising method to produce hydrogen where ultrasound enhances electrolytic process in several ways such as enhanced mass transfer, removal of bubbles and activation of the electrode surface. In this review, production of hydrogen through sonochemical and sonoelectrochemical methods along with a brief description of current hydrogen production methods and power ultrasound are discussed.

Keywords

cavitation; hydrogen; power ultrasound; renewable energy; sonochemistry; sonoelectrochemistry

Table of content

1. Introduction

Fossil fuel resources have been exploited intensively since the beginning of the industrial revolution to meet the ever rising energy demand [1]. Due to the economic development of emerging countries and exponential growth of the human population, there is a substantial pressure on the demand for energy and goods. This lead to an upsurge in fossil fuel consumptions. It is predicted that the global population will increase to 8.9 billion by a factor of 36% and global energy consumption will increase by 77% to 837 quads by 2050 [2]. However, the amount of fossil energy such as coal, hydrocarbons and natural gas on earth is finite. Also, the growth of industrial activities and development of transportation means has resulted in the extremely high emissions of greenhouse gases into the atmosphere. Therefore, it is necessary to explore for pollution free and more efficient energy source in order to replace depleting fossil fuels. Inquest of alternative energy sources has given rise to the concept of The Hydrogen Economy [1]. Hydrogen as an energy source is particularly attractive due to its very high specific energy compared to other conventional fuel types (Table 1).

Hydrogen originating from renewable resources provides clean and sustainable energy produced from local energy sources around the world [2]. It is the simplest and most abundant element in the world, which is readily available as a part of another material (i.e., water, hydrocarbons, and alcohols. Also, hydrogen is available in animals and plants in the form of biomass. Therefore, it is considered more as an energy carrier than energy source [3].

Hydrogen can be produced through different processing technologies such as thermal, electrolytic and photolytic processes. The thermal process includes natural gas reforming, renewable liquid and biooil processing, and the gasification of biomass and coal, whereas the electric process is the splitting of water using external energy sources. Through the photocatalytic method, water is splitted using sunlight through biological and electrochemical materials [3]. Around 60 million tons of hydrogen is produced per year and the consumption is increasing by 6% annually [1], [3]. Currently, 50% of global hydrogen demand is produced by steam reforming of natural gases which releases vast amount of greenhouse gases. Also, 30, 18 3.9 and 0.1 % of hydrogen is produced from oil reforming, coal gasification, water electrolysis and other resources respectively [1], [3]. The primary concern for hydrogen production lies in the development of alternative technologies than traditional methods [3]. The alternative technologies should be highly efficient,

129 environmentally friendly and economical. Sonolysis could be a promising technique to produce
130 clean hydrogen, especially if the hydrogen carrier is solely water [4].

131 *Table 1: Specific energy and energy density of different fuel types*

Fuel types	Specific energy (MJ/kg)	Energy density (MJ/L)	Reference
Diesel	45.6	38.6	[5]
Gasoline	46.4	34.2	[5]
Kerosene	42.8	33	[5]
LPG(propane)	49.6	25.3	[5]
Crude oil	46.3	37	[6]
Heating oil	46	37.4	[6]
Ethanol	29.7	23.4	[7]
Methanol	22.7	17.85	[7]
Butanol	36.1	29.2	[7]
Coal-Black	27.9	-	[6]
Coke	28.0	-	[6]
Wood	14	-	[6]
Natural gas	53.6	-	[6]
Methane	55.6	23.53	[7]
Hydrogen(Liquid)	141.86 (HHV), 119.93(LHV)	10.044(HHV), 8.491(LHV)	[8]
Hydrogen(at 690 bar, and 15°C	141.86(HHV), 191.93(LHV)	5.323(HHV), 4.500(LHV)	[8]
Hydrogen gas	141.86(HHV), 191.93(LHV)	0.01188(HHV), 0.01005(LHV)	[8]

132

133 Hydrogen production using ultrasonication in addition to catalysis, photocatalysis, digestion
134 sludge and anaerobic fermentation of wastewater has been demonstrated to be enhanced compared
135 to the individual methods without ultrasonication [9]. Currently, few studies are available
136 concerning the sonochemical production of hydrogen, and the influence of different operational
137 parameters on hydrogen production is still unclear. Moreover, the coupling of ultrasound with
138 electrochemistry, a newly introduced branch of electrochemistry named as sonoelectrochemistry,
139 could be an advantageous method for hydrogen production by water electrolysis [10].
140 Ultrasonication can enhance mass transfer and in activation of the working electrode surface.

These effects can provide an acceleration of electrochemical processes which ultimately enhances electrochemical production of hydrogen [11].

In this review, an introduction the power ultrasound, hydrogen production through sonochemical and sonoelectrochemical methods along with a short overview of the traditional hydrogen production techniques is presented.

1.1 Current hydrogen production methods

Currently, hydrogen is produced from different energy sources such as nuclear, natural gas, coal and biomass. Renewable resources for hydrogen production are solar, wind, hydroelectric and geothermal energy. In thermal processing, the primary methods are gas reforming, renewable liquid and biooil processing, biomass and coal gasification [3]. The conventional hydrogen production methods are summarized in Figure 1. In this section, a brief description of all these processing technologies is given.

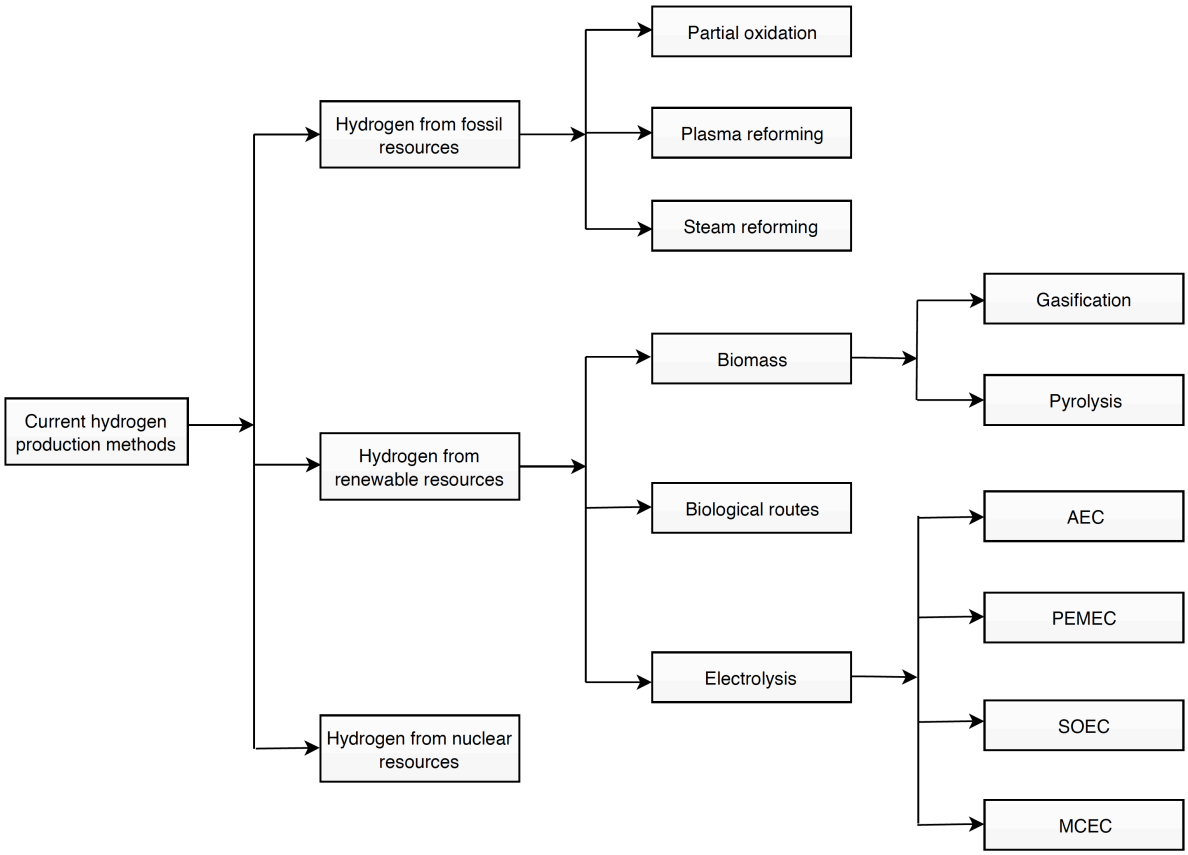

Figure 1: Conventional hydrogen production routes

1.1.1 Hydrogen from fossil resources

Hydrogen-containing materials derived from fossil fuel such as gasoline, hydrocarbons, methanol, and ethanol can be converted into a gas stream rich in hydrogen. Currently, production of hydrogen from natural gas is the most common method. There are three basic methods for hydrogen production from fossil fuels. They are (i) steam reforming, (ii) partial oxidation and (iii) autothermal reforming [3].

1.1.1.1 Steam reforming

One of the most widely used and economical processes for hydrogen production is steam reforming [12]. The process is highly efficient with low operating and production costs. Natural gas, lighter hydrocarbons and methanol are the most frequently used materials for steam reforming [13]. The steam reforming reaction of methane occurs according to reaction (1) and (2).

$$CH_4 + H_2O \rightarrow CO + 3H_2 \qquad \Delta H = +206 \text{ kJ/mol} \quad \text{at } 25°C \qquad (1)$$

$$CH_4 + 2H_2O \rightarrow CO_2 + 4H_2 \qquad \Delta H = +165 \text{ kJ/mol} \quad \text{at } 25°C \qquad (2)\ [1]$$

Both reactions (1) and (2) are very endothermic. Therefore, methane reforming has to be carried out at very high temperature (i.e., 1000°C over a heterogenous catalysts) [1]. The overall process consists of two stages. Hydrocarbons are mixed with steam in the presence of metal catalyst in the first stage. This process produces syngas (a mixture of H_2 and CO), where CO is around 20 wt.% [1], [14] with small amount of CO_2 [14]. For further use of H_2, the CO has to be removed from the syngas. In the second stage of the process, CO is removed through the water gas shift (WGS) reaction (3) [1], [12].

$$CO + H_2O(g) \leftrightarrow CO_2 + H_2 \qquad \Delta H = -41 \text{ kJ/mol} \quad \text{at } 25°C \qquad (3)\ [1]$$

This reaction is exothermic. Therefore, WGS reaction has to be carried out at lower temperature in the range of 200 to 350°C [1]. Hydrogen production by steam reforming of methanol is carried out in moderate temperature ca. 180°C (4) [3].

$$CH_3OH + H_2O(g) \leftrightarrow CO_2 + 3H_2 \qquad (4)\ [3]$$

Both precious (Pt, Rh) and non-precious (Ni) metals are used as catalysts for steam reforming. An important factor in the steam reforming process is the H:C atom ratio in the feedstock material. The higher the ratios are the lower CO_2 content is formed [3]. The heat efficiency of hydrogen production by methane reforming is around 70-85% in industrial scale [15]. The main disadvantage of this process is the high production of CO_2 (ca., 7.05 kg CO_2/ kg H_2) [3]. Despite this, fossil fuel based hydrogen production routes have higher efficiency, but the high emission of

188 CO_2 is a huge drawback for this production methods. Table 2 summarizes the CO_2 emission from
189 different fossil fuel-based hydrogen production methods.
190 Steam-reforming of ethanol can produce hydrogen according to the following reactions.

191 $$CH_3CH_2OH + H_2O \rightarrow 2CO + 4H_2 \qquad \Delta H_{298}^{0} = +255 \text{ kJ/mol} \quad \text{at } 25°C \qquad (8)$$

192 $$CH_3CH_2OH + 3H_2O \rightarrow 2CO_2 + 6\,H_2 \qquad \Delta H_{298}^{0} = +173 \text{ kJ/mol} \quad \text{at } 25°C \qquad (9)[1]$$

193 Both these reactions are endothermic. Therefore, they need to be carried out in high temperature
194 as well as in low pressure due to the increase of the number of moles in the in the steam reforming
195 reactions. However, in low-pressure and high temperature condition various side reactions can
196 develop. Some of those side reactions produce hydrogen.

197 $$CH_3CH_2OH \rightarrow CH_3CHO + H_2 \qquad \Delta H_{298}^{0} = +68 \text{ kJ/mol} \qquad (10)$$

198 $$CH_3CH_2OH \rightarrow CH_4{+}CO{+}H_2 \qquad \Delta H_{298}^{0} = +49 \text{ kJ/mol} \qquad (11)$$

199 $$CH_3CH_2OH \rightarrow C{+}CO{+}3H_2 \qquad \Delta H_{298}^{0} = +124 \text{ kJ/mol} \qquad (12)[1]$$

200 The efficiency of ethanol steam-reforming can be improved by using catalysts. Ni/Al_2O_3 and
201 Rh/Al_2O_3 are employed successfully for ethanol reforming at 700°C. It was observed that
202 Rh/Al_2O_3 is more active than Ni/Al_2O_3, the yield of hydrogen is eight times higher with Rh than
203 with Ni, with respect to the mass of the metal. CeO_2- ZrO_2 based mixed oxide catalysts can
204 overcome this problem showing excellent stability and high activity [1].
205
206 *Table 2: CO_2 emission and energy consumptions from different fossil fuel based hydrogen production.*

Processing technology	Fuel types	CO_2 emission kg CO_2/kg_H_2	Energy consumption MJ/kg_H_2	Efficiency %	Ref.
Steam reforming	CH_4	7.05	165	70-85	[15]–[17]
	Natural gas	10.621	159.6	89.3	[18]
Plasma Reforming	CH_4	negligible	45-55	90-100	[19]
Methanol cracking	CH_3OH	14.45	-	95	[20], [21]
Gasification	Coal	31.09	271	44.3	[17], [22], [23]
Gasification	Biomass	3.96	242	48.3	[3], [17], [22], [24]

207

1.1.1.2 Partial oxidation

Hydrogen production from hydrocarbons through partial oxidation and catalytic partial oxidation is another promising method for hydrogen production [25], [26]. The primary raw material has a heavy oil fraction that is difficult to treat for further utilization. Methane and biogas can also be used as raw materials [27]. In partial oxidation, the gasification of the raw material is carried out in the presence of oxygen and steam at elevated temperature (In the range of 1300-1500°C) and pressure (3-8 MPa) [28].

$$CH_4 + O_2 \rightarrow CO + 2H_2 \quad (5)$$

$$CH_4 + 2O_2 \rightarrow CO_2 + 2H_2O \quad (6)$$

$$CH_4 + H_2O(g) \rightarrow CO + 3H_2 \quad (7)\ [28]$$

The partial oxidation products of hydrocarbon are CO, CO_2, H_2O, H_2, CH_4, H_2S and COS. A part of this gas is burned to provide additional heating for the endothermic partial oxidation process. Partial oxidation is less expensive than steam reforming but the subsequent conversion makes the process more expensive. By adding a catalyst, the operating temperature can be lowered to 700-1000°C [3]. The typical catalysts used in partial oxidations is Ni or Rh; however, they have a disadvantage of forming coke [26]. Therefore, modification of a Ni catalyst can be performed by using Mg to decrease coke formation. Mg modified Ni catalysts inhibit dehydrogenation of absorbed CH_x and enhances the steam adsorption. Using noble metals also prevents formation of coke [29]. The typical thermal efficiency of partial oxidation with methane is in the range of 60-75% [30].

Another hydrogen production method is autothermal reforming (ATR), a combination of steam reforming and partial oxidation where steam is introduced in the catalytic partial oxidation process [31]. ATR is a simpler and less expensive process than steam reforming, and it is more favorable for not requiring external heating [3]. Another advantage of ATR over SR is the rapid shutting down of the equipment [31]. The thermal efficiency of methane reforming is comparable to partial oxidation (60-75%) [32].

Plasma reforming is another promising method to produce hydrogen from hydrocarbons. The formation of plasma reforming reactions is identical to the steam reforming reactions. In plasma reforming, the formation of free radicals and required energy are provided by plasma [3]. Hydrogen can be produced in plasma reformers from various hydrocarbon fuels (e.g., gasoline, diesel, oil, biomass, natural gas and jet fuels), with a conversion efficiency near 100% [19], [33].

The high degree of dissociation, high temperature and substantial degree of ionization of plasma can promote chemical reactions even in the absence of a catalyst [3]. There are numerous advantages for using a plasma reformer over conventional reformers. They are compact, low weight, have high conversion efficiencies, lower costs, and have a fast response time operation with various fuels. Dependency on electricity and the difficulty of having a in high-pressure operation are the major disadvantages of plasma reforming [34] .

1.1.2 Hydrogen from renewable resources

Hydrogen can be produced from renewable resources instead of reforming fossil fuels. Biomass based approaches and water electrolysis are the primary sources of renewable hydrogen [3]. In this section, a brief description of hydrogen production from renewable resources is given.

1.1.2.1 Hydrogen from biomass gasification and pyrolysis

Biomass is an excellent renewable source of energy and chemicals. It can be available in different form such as animal wastes, municipal solid wastes, crop residue, agricultural waste, sawdust, aquatic plants, waste paper and corn [35], [36]. Gasification is a widely used technology where biomass and coal are used as a fuel feedstock in many commercially available processes. In gasification, biomass is partially oxidized into a mixture of hydrogen, methane, carbon dioxide, carbon monoxide and higher hydrocarbons named as ´producer gas´ [35]. The process is the combined results of many heterogeneous and homogeneous reactions [37]. The maximum yield of hydrogen from lignocellulosic biomass is 17 wt.% through steam gasification based on biomass weight [2]. A straightforward method for hydrogen production from biomass is oxygen or air gasification followed by the water-gas shift reaction. Based on the following reactions, the stoichiometric yield of hydrogen production from typical biomass is 14.3 wt.% [2].

$$CH_{1.46}O_{.67} + 0.16O_2 \rightarrow CO + 0.73H_2 \quad (13)$$

$$CO + H_2O \leftrightarrow CO_2 + H_2 \quad (14)$$

$$CH_{1.46}O_{.67} + 0.16O_2 + H_2O \rightarrow CO_2 + 1.73H_2 \quad (15)\ [2]$$

During the gasification process, a small amount of biomass carbon is converted into char, tar and CO_2. This results in less amount of CO for water-gas shift reaction. Therefore, the practical yield is less than the theoretical yield [2].

Biomass can be gasified through supercritical water (220 bar and 374°C) into a product gas containing H_2 and CO_2 [38]. The reaction can be presented as below.

$$CH_x O_y + (2\text{-}y)H_2O \rightarrow CO_2 + \frac{2-y+x}{2} H_2 \quad (16)\ [38]$$

The main advantage of this approach is that the biomass does not need to be dried, which is a very energy intensive process [37]. In addition, gasification can be carried out efficiently at low temperatures which is below 700°C. Another advantage is the high-pressure product hydrogen which reduces the energy cost significantly for compression during storage [39]. On the other hand, this technology experiences some disadvantages such as corrosion and plugging as well as the requirement of external energy input for preheating both the biomass and the reactor [37].

Another promising method for hydrogen production is pyrolysis and reforming. It is a two-step process where pyrolysis of biomass is carried out in the first step. After that the pyrolysis undergoes a catalytic steam reforming process [2]. Biomass is heated and gasified at a pressure of 1-5 bar and temperature 500-900°C in the absence of oxygen or air, which avoids the formation of CO or CO_2 as well as the need for the WGS reactions. This process can be divided into three categories depending on the operating temperature range such as low (up to 500°C), medium (500-800°C) and high (over 800°C) [3]. Fast pyrolysis through high heat transfer can maximize the formation of volatile intermediate compounds. Fluidized bed and entrained flow reactors are in commercial use for fast pyrolysis of biomass. The composition of the pyrolysis oil depends on the reaction conditions, reactor types and raw materials [2]. Based on the following stoichiometry, hydrogen yield through pyrolysis can reach up to 13%, which is comparable with gasification [40].

$$\text{Biomass} \rightarrow \text{Bio-oil} + \text{Char} + \text{Gas} \quad (17)$$

$$CH_{1.46}O_{0.67} \rightarrow 0{:}\ 71CH_{1.98}O_{0.76} + 0.21CH_{0.1}O_{0.15} + 0.08CH_{0.44}O_{1.23} \quad (18)$$

$$CH_{1.98}O_{0:76} + 1.24H_2O \rightarrow CO_2 + 2.23H_2 \quad (19)\ [40]$$

1.1.2.2 Hydrogen production through biochemical routes

Production of hydrogen through biological routes offers a wide range of approaches. The major production routes are direct and indirect biophotolysis, photo-fermentation and dark fermentation [41]. Via direct photolysis, water molecules are split into hydrogen ion and oxygen by algae through photosynthesis. Hydrogenase enzymes converts the hydrogen ions into hydrogen gas. The eukaryotic algae *Chlamydomonas reinhardtii* is a widely used algae for hydrogen production [42]. This approach could be considered as economical and sustainable due to water utilization as a renewable resource and CO_2 consumption by the algae. However, generated oxygen provides a strong inhibition effect on hydrogenase enzymes which is a major limitation of the process. On the

other hand, through indirect photosynthesis, cyanobacteria can produce hydrogen according to equation (20) and (21).

$$12H_2O + 6CO_2 \xrightarrow{Light\ energy} C_6H_{12}O_6 + O_2 \quad (20)$$

$$C_6H_{12}O_6 + 12\ H_2O \xrightarrow{Light\ energy} 12\ H_2 + 6\ CO_2 \quad (21)\ [41]$$

Cyanobacteria contain several enzymes that take part in hydrogen metabolism and produce molecular hydrogen. They are mainly nitrogenases and hydrogenases. Nitrogenases contributes in catalyzing the production of hydrogen, which is a byproduct of nitrogen reduction to ammonia, whereas the hydrogenases catalyze the oxidation of hydrogen produced by nitrogenases [41].

Dark and photo-fermentation are considered to be more auspicious than algal hydrogen production as they can simultaneously perform waste treatment and hydrogen production. Dark fermentation is the process where the organic compounds that produce hydrogen are the only metabolic energy sources [43]. The yield of hydrogen production is mostly based on hexose conversion where the maximum theoretical yield of hydrogen is 4 mol from 1 mol of glucose consumed.

$$C_6H_{12}O_6 + 4H_2O \rightarrow 2CH_3COO^- + 2HCO_3^- + 4H^+ + 4H_2 \quad \Delta G'_0 = -206\ kJ/mol. \quad (22)\ [43]$$

Dark fermentation for hydrogen production can be carried out through mixed acidogenic microbial culture obtained mainly from soil or waste water sludge. They work in different temperature regions such as mesophilic (25°C - 40°C), thermophilic (40°C – 65°C), extreme thermophilic (65°C – 80°C) and hyperthermophilic (> 80°C). There is a number of microorganisms used for hydrogen production. The most widely studied bacteria for hydrogen production are *Clostridia, and Enterobacter* species. The thermophiles and hyperthermophiles are favorable for hydrogen production from biomass due to elevated reaction kinetics at a higher temperature. The main influencing parameters in dark fermentation are organic loading, pH, temperature, hydraulic retention time (HRT) and gas stripping to avoid high partial hydrogen pressure [43].

Photo-heterotrophic bacteria can produce hydrogen in the presence of light from organic acids under anaerobic condition. Therefore, the organic acids that are produced during the acidogenic stage of anaerobic conditions can be transformed into hydrogen and carbon dioxide by photosynthetic anaerobic bacteria. A schematic diagram of hydrogen production from lignocellulosic biomass is given in Figure 2. The investigated photosynthetic purple bacteria include *Rhodobacter spheroids, Rhodobacter capsulatus, Rhodovulum sulfidophilum* and *Rhodopseudomonas palustris.* The optimum operating temperature for photosynthetic bacteria is

in the range of 30-35°C and pH 7.0 [42]. The fermentation is carried out in anaerobic conditions under light illumination. The hydrogen production rate depends on the light intensity, the type of microbial culture and carbon source. The primary enzyme that catalyzes hydrogen production by photosynthetic bacteria is the nitrogenase. The presence of oxygen, ammonia or at high N/C ratio inhibits the activity of the nitrogenase enzyme. Therefore, oxygen free and limited ammonium conditions are favorable for the process [42].

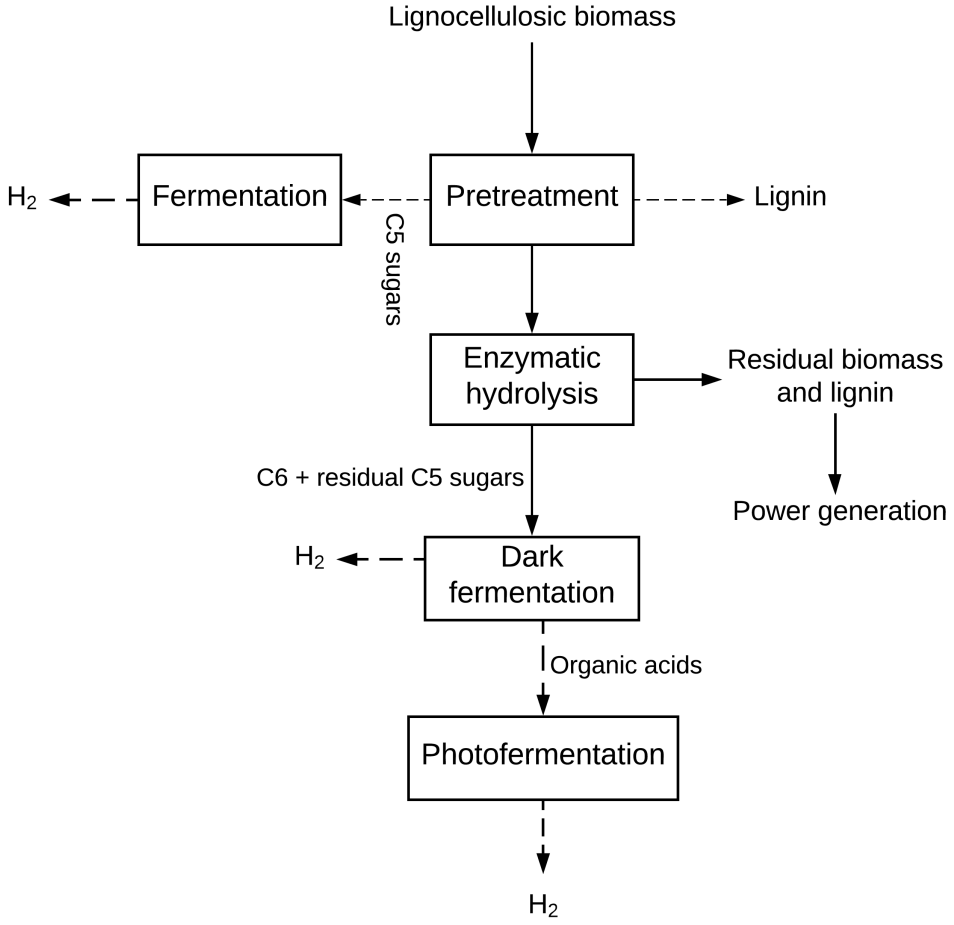

Figure 2: A schematic diagram of hydrogen production from lignocellulosic biomass

1.1.2.3 Hydrogen from water electrolysis

Hydrogen production through water electrolysis could be a promising method in future. Currently, about 4% of total hydrogen production is obtained through water electrolysis [44]. Electrolysis is a process where direct current is passed through two electrodes in aqueous solution [3]. The two electrodes are anode and cathode where oxidation and reduction of water occur respectively

producing oxygen and hydrogen [1], [3]. Based on the electrolytes and working temperature, electrolysis of water can be divided into four main catagories:

- Alkaline electrolysis cell (AEC): In this kind of cell, the ionic species are the hydroxyl group (OH^-), with aqueous KOH or NaOH as electrolytes at a working temperature below 80°C [1].
- Proton Exchange Membrane Electrolysis Cell (PEMEC): In PEMEC, the ionic species are hydrogen ion (H^+), with perfluorosulfonic acid (PFSA) membranes as solid electrolytes and at a working temperature below 80°C [1].
- Solid oxides electrolysis cell (SOEC): In SOEC, the ionic species are oxide ions (O^{2-}), with yttrium-stabilized zirconia as solid electrolytes, and a working temperature above 700°C [1].
- Molten Carbonate Electrolytic Cell (MCEC) : In MCEC, the ionic species are carbonate ions (CO_3^{2-}), with molten sodium and potassium carbonate as electrolyte, and the working temperature is in the range of 600-700°C with an operating pressure 1-8 atm [45].

The mechanism of different electrolyzers for hydrogen production is illustrated in Figure 3. The half-reactions that occur in the different types of water electrolyzer are as follows.

In AEC;

$$\text{Cathodic reaction: } 2H_2O\,(l) + 4e^- \rightarrow 2H_2\,(g) + 4OH^-\,(aq) \quad (23)$$

$$\text{Anodic reaction: } 4OH^-\,(aq) \rightarrow O_2\,(g) + 2H_2O(l) + 4e^- \quad (24)$$

In PEMEC;

$$\text{Cathodic reaction: } 4H^+ + 4e^- \rightarrow 2H_2 \quad (25)$$

$$\text{Anodic reaction: } 2H_2O \rightarrow 4H^+ + 4e^- + O_2 \quad (26)$$

In SOEC;

$$\text{Cathodic reaction: } 2H_2O + 4e^- \rightarrow 2H_2 + 2O^{2-} \quad (27)$$

$$\text{Anodic reaction: } 2O^{2-} \rightarrow O_2 + 4e^- \quad (28)$$

In MCEC;

$$\text{Cathodic reaction: } H_2O + 2CO_2 + 2e^- \rightarrow H_2 + CO_3^{2-} \quad (29)$$

$$\text{Anodic reaction: } CO_3^{2-} \rightarrow 1/2O_2 + CO_2 + 2e^- \quad (30)$$

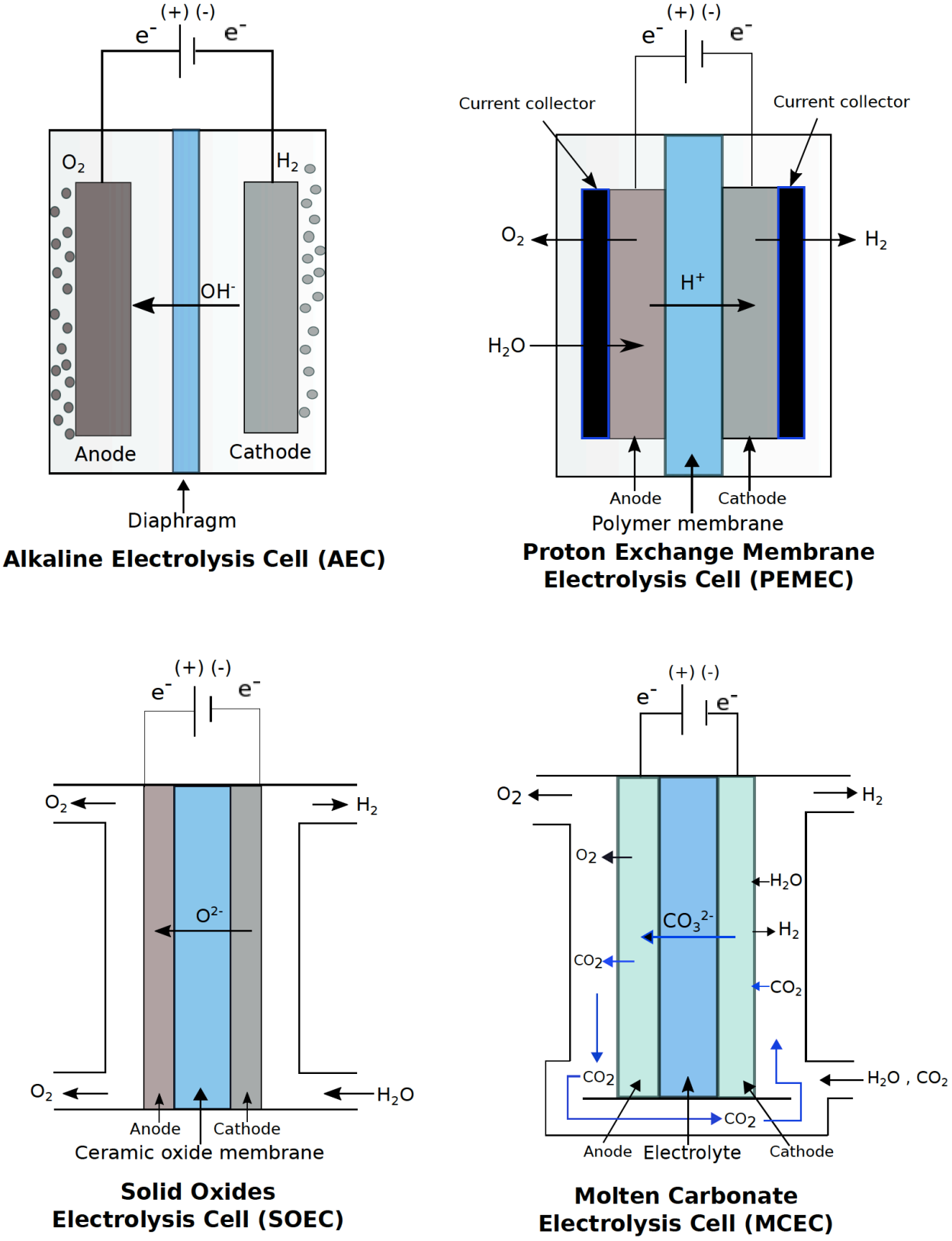

Figure 3: Mechanism of different electrolyzer for hydrogen production

To produce 1 kg of hydrogen, 39 KWh of electricity and 8.9 liters of water is required at a temperature of 25°C, with 1 atmospheric pressure (if run at 100% efficiency of the theoretical reaction kinetics). Typical commercially available electrolyzers have efficiencies around 56-73 % where 53.4-70.1 kWh of electricity is required to produce 1 kg of hydrogen [46].

The alkaline electrolyzer or the AEC is the most widely used electrolyzer for hydrogen production. Typically, 20-30 wt.% of potassium hydroxide (KOH) aqueous solution is used as the electrolyte. Porous nickel electrode is the most widely used electrode in these types of cells [47]. Commercially available AEC´s are run with current densities in the range of 100-300 $mAcm^{-2}$ [2]. The main drawback of this technology is the profound purity of hydrogen caused by cross diffusion of hydrogen and oxygen between the electrodes. This causes safety issues related to hydrogen explosion [48]. The bubbles cannot be removed rapidly during water electrolysis. The accumulation of bubbles on the electrode surfaces and dispersion of bubbles in the electrolyte can lead to a high ohmic voltage drop and a large reaction overpotential. One of the vital points for high consumption of energy is the bubble effect in water electrolysis [49]. It was observed that ultrasound could diminish the bubble effect as well as remove bubbles from the electrolyte which ultimately enhances the electrochemical process. Details of this phenomena are discussed in section 1.3 and 1.4.

In PEMEC, a solid proton-conductive but electronically nonconductive membrane is used, where the membrane serves as gas separation device and ion conductor [47]. High purity water is needed for PEMEC based electrolysis, and 1 MΩ-cm resistive water is recommended to extend stack life. DI water is introduced at the anode of the cell. To dissociate the water , a potential is applied across the cell. Due to the electric field, the protons are passed through the membrane and form hydrogen gas at the cathode. They are operated at high current densities (higher than 1600 $mAcm^{-2}$), which increases the hydrogen production rate [2]. In addition, PEMEC can produce high purity hydrogen gas through preventing gas diffusion by the solid polymer membrane. This technology is well established with efficiency ranging from 48% to 65% [50]. However, due to the low stability of noble metal based electrocatalysts and high capital cost, the commercialization of PEMEC is limited [47].

The least developed but most efficient electrolyzers are the SOEC [3]. In this electrolyzer, steam is oxidized to produce hydrogen at the hydrogen electrode . The O^{2-} migrates through yttria-stabilized zirconia (YSZ) to the oxygen electrode to produce pure oxygen. The efficiency of SOEC

can reach up to ~90% [51]. The SOEC is still in the early stage of development compared to AEC and PEM. Nevertheless, it is a promising technology for hydrogen production in large scale due to its high efficiency and low costs, avoiding the use of expensive noble metal catalysts [47].

Molten carbonate fuel cells (MCFC) are the most recently developed electrolyzer for producing hydrogen. MCFCs are promising option to produce hydrogen via water electrolysis, syngas, and co-electrolysis of water and carbon dioxide. MCFCs operate as a molten carbonate electrolysis cell (MCEC) when it is run in reverse. The anode of MCFC, which is a nickel electrode, works as a cathode in MCEC where hydrogen evolution occurs. A mixture of NiO and Li_2O is used as an anode where oxygen evolution occurs [52]. The overall reaction in MCEC is presented in equation (31).

$$H_2O + CO_2 \rightarrow H_2 + \frac{1}{2}O_2 + CO_2 \qquad (31)\ [52]$$

A mixture of lithium and potassium or lithium and sodium carbonates are used as the electrolyte. However, MCEC is not preferable for producing pure hydrogen, as carbon- dioxide is involved in the reactions where one mole of CO_2 must be transferred through the electrolyte for producing each mole of hydrogen. The production efficiency of hydrogen and energy consumption of different electrolyzers is summarized in Table 3.

Table 3: Summary of the electrolyzer for hydrogen production

Electrolyzer	Temperature range °C	Energy consumption kWh/kg of H_2	Efficiency %	Ref.
AEC	60-80	53.4-70.1	56-73	[46]
PEMEC	50-80	54.21-90.36	48-65	[48], [50]
SOEC	600-900	26.91	90	[51], [53]
MCEC	600-700	-	90	[52]

1.1.2.4: Hydrogen production by photoelectrolysis

Photocatalysis is an efficient and cost-effective method for hydrogen production from renewable resources [54]. Semiconducting materials are used as the electrode where solar energy is absorbed and simultaneously creating the voltage for hydrogen production through water decomposition. Photoelectrolysis of water is driven by a photoelectrochemical (PEC) light collection system. The type of semiconductor materials and solar intensity is responsible for the photochemical reaction.

The current density produced is in the range of 10-30 mA/cm^2. The necessary voltage at this current density is 1.35 V approximately.

The photoelectrode includes a photovoltaic, catalytic and a protective layer [55]. The overall efficiency of the photoelectrochemical system is influenced by the performance of each layers. Light absorbing semiconductor materials are used in the photovoltaic layer. The performance of the photoelectrode is directly proportional to the light absorption of the semiconductor materials. The performance of the water electrolysis by photoelectrochemical cell is also influenced by the catalytic layers thus requiring a suitable catalysts. The protective layer is another crucial element of the photoelectrode, which protects the semiconductor from corrosion. This layer needs to be highly transparent for providing maximum solar energy to the photovoltaic semiconducting layer [2].

1.2 Power ultrasound

Ultrasound is the acoustic wave that has a frequency above the upper limit of the human hearing range. This range varies from person to person and is approximately above 20 kHz. At a "very high frequency," ultrasound above 1 MHz is called low power ultrasound. The power is normally less than 10 W. Low power ultrasound does not influence the medium of propagation. Therefore, it is used for medical diagnosis or non-destructive material control. In the range between 20 and 100 kHz, waves are defined as "low-frequency ultrasound" or "power ultrasound." Figure 4 demonstrates some typical use of ultrasound according to power and frequency [10], [56].

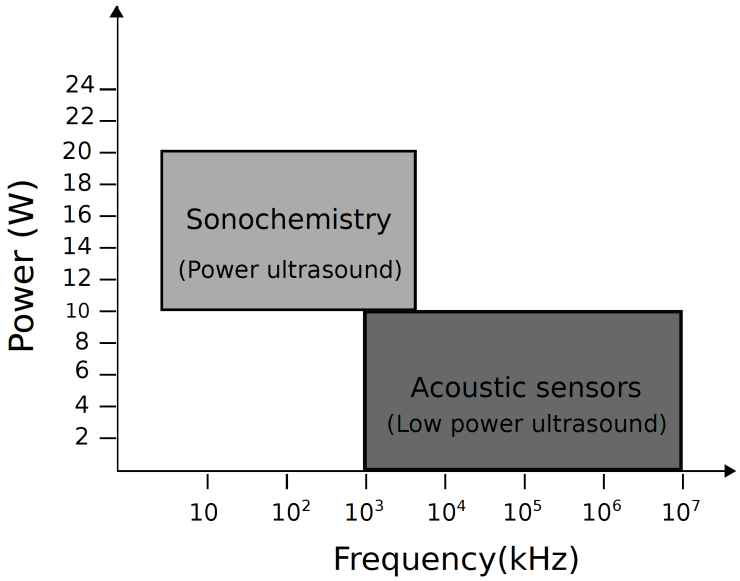

Figure 4: *Utilizations of ultrasound according to frequency and power*

Power ultrasound is transferred at a high power level (a few tens of watts) and therefore able to alter the medium it propagates through. It can disrupt a liquid bulk in order to generate cavitation or acoustic streaming [10], [56]. Power ultrasound can be used in two different ways to bring changes in a material and these are:

i) **Direct transmission:** It is the direct mechanical transmission of vibration from the ultrasound transducer onto a solid surface for inducing vibration.

ii) **Indirect transmission:** Indirect transmission is caused via cavitation into a fluid due to the transmission of acoustic vibrations [10].

Several effects may be induced by ultrasound propagation into a liquid media. Two major effects are acoustic cavitation and acoustic streaming. Acoustic streaming arises from the dissipation of acoustic energy. Other effects may cause by ultrasound are heating due to the dissipation of the mechanical energy and nebulization. High frequency ultrasound causes an acoustic fountain at the liquid-gas interface. A temperature of 250°C can be obtained at this interface [56].

Acoustic cavitation is the most important phenomena that may arise from the propagation of ultrasound wave into a liquid. When ultrasound waves propagate through a liquid media such as water, many tiny gas bubbles form (Figure 5). When the acoustic pressure is higher than the atmospheric pressure, the instantaneous local pressure becomes negative during rarefaction phase of the ultrasonic wave. This "force" allows expanding of a liquid or solid, which is also called "weak spots."

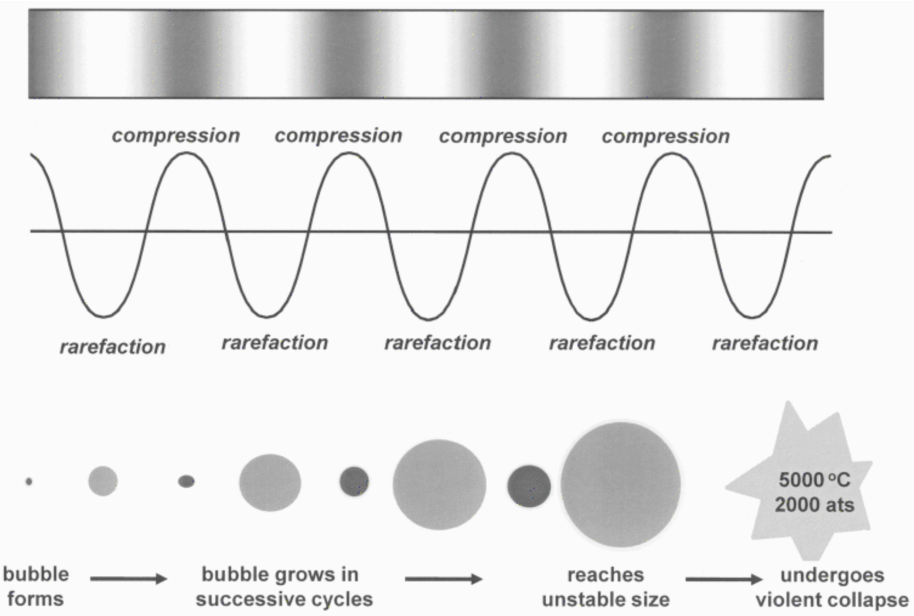

Figure 5: Sinusoidal wave form and bubble collapse [10].

Therefore, the dissolved gases in the liquid come out as gas bubbles as gases cannot be dissolved in the liquid under negative pressure. Those tiny gas bubbles at the rarefaction phase expand due to the higher pressure at the bubble wall rather than the liquid pressure at a distance from the bubble. During the compression phase, some of those bubbles violently collapse leading to shock waves [57]. The number of bubbles generated during the rarefaction cycle is proportional to the density of weak spots present in the liquid media [58]. The phenomenon of formation of bubbles and their subsequent violent collapse of the bubbles is known as acoustic cavitation [57]. In aqueous media, each cavitation bubble acts as a local "hotspot," which generates a temperature of 5000°C and pressure of 500 atmospheres [59] . The bubble collapse occurs with a collision density of 1.5 $kgcm^{-2}$ and pressure gradients of 2 $TPacm^{-1}$. The collapsing of bubbles imparts both chemical and mechanical effects into the aqueous media. The chemical effect is experienced inside the bubble, which can be considered as a high pressure and high temperature microreactor. A massive shear force caused by the shockwave due to bubble collapse will be experienced in the immediate vicinity of the bubbles [10].

1.3 Sonochemistry

Sonochemistry is a relatively new concept that received attention in the late 1970s. In the beginning, it was defined as the application of ultrasound in chemistry. The significant effects caused by acoustic cavitation is the Sonochemistry and Sonoluminesence [60]. Sonochemical reactions can take place under single or multibubble cavitation. The latter is the dominant one as sonochemical reactions in an ultrasonic bath or with horns are always multibubble phenomena. As mentioned earlier, very high temperature and pressure is generated during cavitation bubble collapse. The cavitation bubble contains gas molecules such as N_2 and O_2 and vapor from the solvent. In the high temperature and pressure generated by bubble collapse, the solvent vapor and gas molecules generate various highly reactive radicals such as OH radicals, O_3, H_2O_2 and O atoms through endothermic chemical reactions [Figure 6] [57], [60]. These oxidants diffuse out from the interior of the bubble into the surroundings and react with solutes present in the aqueous solution [57]. OH radicals are the most dominant oxidant in sonochemical reactions. The production of O_3 is negligible comparing to OH radicals and O atoms reacts with H_2O to produce H_2O_2 [61]. The oxidation-reduction potential of OH• (2.06 V) is much higher than that of H_2O_2 (1.776 V). Therefore OH• plays more critical role in sonochemical reactions than H_2O_2 [62]. Near the bubble wall, the concentration of hydroxyl radical is about 5×10^{-3} M. The life time of these are about 20

ns when the initial concentration is 5 x 10^{-3} M and is determined by the reaction between them in the absence of solutes as presented in equation (32) [63].

$$OH\bullet + OH\bullet \rightarrow H_2O_2 \qquad (32)$$

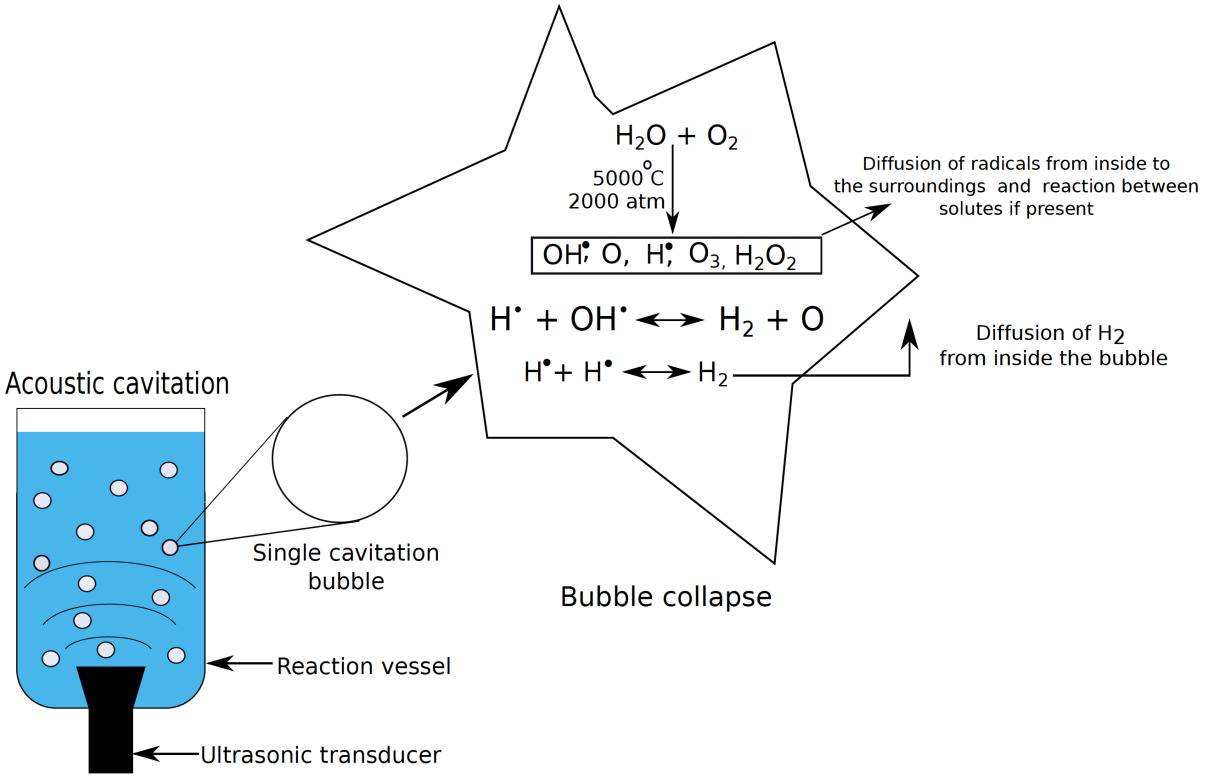

Figure 6: Production of oxidants by acoustic cavitation.

Several factors affect the sonochemical reactions. Among them, the ultrasonic frequency is the dominant factors that should be taken into account to obtain maximum efficiency in sonochemical reactions. The mechanical forces exerted by sonication are directly dependent on ultrasonic frequency. The lower frequency provides the largest mechanical effect. Another major factor that dominates the sonochemical reactions is acoustic power or intensity. By using a standard calorimetric method, the acoustic power absorbed by a liquid can be determined as stated in equation (33).

$$q = m*C*\Delta T \qquad (33)\ [60]$$

where q = heat in joules, m = mass of water in grams, C = specific heat capacity of water and ΔT = temperature difference. It is observed that with increasing acoustic power, the production of

hydrogen peroxide increases (Figure 7) [60]. In addition, the number of active bubbles and the bubble size is also expected to increase with increasing acoustic power at a given frequency.

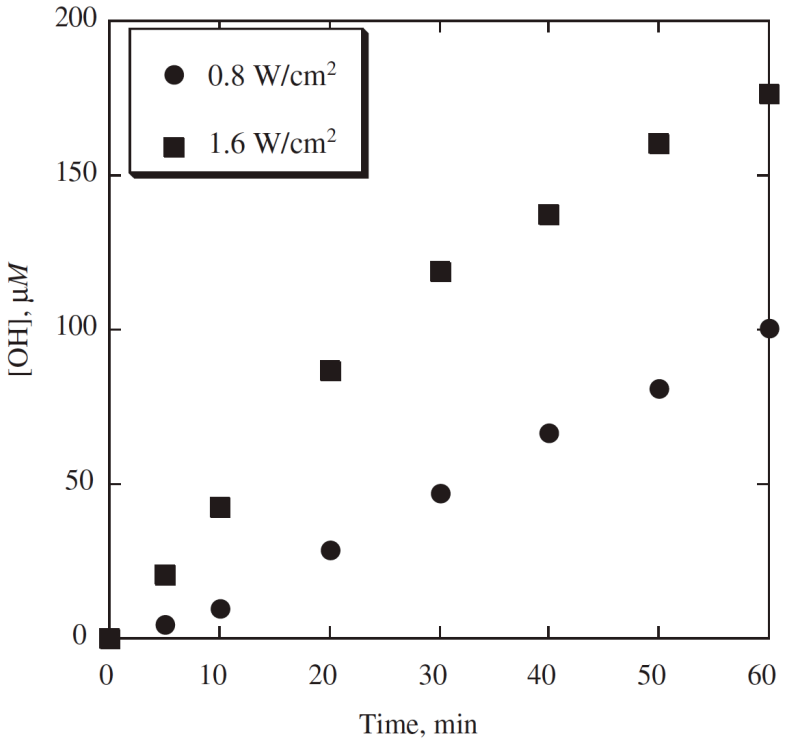

Figure 7: The production of OH radicals as a function of time at different acoustic intensity [60].

Another significant factor affecting the formation of radicals is the type of dissolved gases in the reaction media. Mason [60] has stated that maximum temperature generated at cavitation bubbles collapse depends on the types of dissolved gases. The amount of primary radicals formed by cavitation is the same with any of the noble gases. However, the thermal conductivity of the noble gases decreases with increasing atomic weight. As helium has the lowest atomic weight, more heat will be dispersed to the surrounding from the bubble. Therefore, a helium saturated aqueous solution has a lower maximum bubble temperature leading to a lower primary radical formations. The presence of oxygen is crucial for some sonochemical reactions. If air saturated water is sonicated, then reactions involving O_2 and N_2 may occur. Possible sonochemical reactions by acoustic cavitation are presented in (Table 4). The generation of NO_2 leads to the formation of nitric acid, which decreases the pH of water [60].

The bulk solution temperature influences the sonochemical reactions in several ways. The vapor pressure, as well as the internal pressure within the collapsing bubbles, increases with increasing

538 *Table 4: List of the possible sonochemical reaction inside a collapsing bubble. Here M is third body. The*
539 *subscript "f" stands for forward reaction and "r" stands for reverse reaction. A is in (cm^3 $mol^{-1}s^{-1}$) and*
540 *Ea is in (cal mol^{-1})* [64].

N	Reaction	A_f	b_f	E_{af}	A_r	b_r	E_{ar}
1.	$H_2O + M \leftrightarrow H + OH + M$	1.912×10^{23}	1.83	1.185×10^5	2.2×10^{22}	2.0	0.0
2.	$O_2 + M \leftrightarrow O + O + M$	4.515×10^{17}	0.64	1.189×10^5	6.165×10^{15}	0.5	0.0
3.	$OH + M \leftrightarrow O + H + M$	9.88×10^{17}	0.74	1.021×10^5	4.714×10^{18}	1.0	0.0
4.	$H + O_2 \leftrightarrow O + OH$	1.915×10^{14}	0.0	1.644×10^4	5.481×10^{11}	0.39	2.93×10^2
5.	$H + O_2 + M \leftrightarrow HO_2 + M$	1.475×10^{12}	0.6	0.0	3.09×10^{12}	0.53	4.887×10^4
6.	$O + H_2O \leftrightarrow OH + OH$	2.97×10^6	2.02	1.34×10^4	1.465×10^5	2.11	2.904×10^3
7.	$HO_2 + H \leftrightarrow H_2 + O_2$	1.66×10^{13}	0.0	8.23×10^2	3.164×10^{12}	0.35	5.551×10^4
8.	$HO_2 + H \leftrightarrow OH + OH$	7.079×10^{13}	0.0	2.95×10^2	2.027×10^{10}	0.72	3.684×10^4
9.	$HO_2 + O \leftrightarrow OH + O_2$	3.25×10^{13}	0.0	0.0	3.252×10^{12}	0.33	5.328×10^4
10.	$HO_2 + OH \leftrightarrow H_2O + O_2$	2.89×10^{13}	0.0	4.97×10^2	5.861×10^{13}	0.24	6.908×10^4
11.	$H_2 + M \leftrightarrow H + H + M$	4.577×10^{19}	1.4	1.044×10^5	1.146×10^{20}	1.68	8.2×10^2
12.	$O + H_2 \leftrightarrow H + OH$	3.82×10^{12}	0.0	7.948×10^3	2.667×10^4	2.65	4.88×10^3
13.	$OH + H_2 \leftrightarrow H + H_2O$	2.16×10^8	1.52	3.45×10^3	2.298×10^9	1.40	1.832×10^4
14.	$H_2O_2 + O_2 \leftrightarrow HO_2 + HO_2$	4.634×10^{16}	0.35	5.067×10^4	4.2×10^{14}	0.0	1.198×10^4
15.	$H_2O_2 + M \leftrightarrow OH + OH + M$	2.951×10^{14}	0.0	4.843×10^4	1.0×10^{14}	0.37	0.0
16.	$H_2O_2 + H \leftrightarrow H_2O + OH$	2.410×10^{13}	0.0	3.97×10^3	1.269×10^8	1.31	7.141×10^4
17.	$H_2O_2 + H \leftrightarrow H_2 + HO$	6.025×10^{13}	0.0	7.95×10^3	1.041×10^{11}	0.70	2.395×10^4
18.	$H_2O_2 + O \leftrightarrow OH + HO$	9.550×10^6	2.0	3.97×10^3	8.66×10^3	2.68	1.856×10^4
19.	$H_2O_2 + OH \leftrightarrow H_2O + HO_2$	1.0×10^{12}	0.0	0.0	1.838×10^{10}	0.59	3.089×10^4
20.	$O_2 + O + M \leftrightarrow O_3 + M$	4.1×10^{12}	0.0	2.114×10^3	2.48×10^{14}	0.0	2.286×10^4
21.	$OH + O_2 + M \leftrightarrow + O_3 + H$	4.4×10^7	1.44	7.72×10^4	2.3×10^{11}	0.75	0.0
22.	$O_3 + H \leftrightarrow HO_2 + O$	4.1×10^{12}	0.0	2.114×10^3	-	-	-
23.	$O_3 + O \leftrightarrow O_2 + O_2$	5.2×10^{12}	0.0	4.18×10^3	-	-	-
24.	$O_3 + OH \leftrightarrow O_2 + HO_2$	7.8×10^7	0.0	1.92×10^3	-	-	-
25.	$O_3 + HO_2 \leftrightarrow O_2 + O_2 + OH$	1.0×10^{11}	0.0	2.82×10^3	-	-	-
H/O/N reactions							
26.	$N_2 + M \leftrightarrow N + N + M$	3.7×10^{21}	1.6	2.264×10^5	3.0×10^{14}	0.0	1.0×10^3
27.	$N_2 + O_2 \leftrightarrow N_2O + O$	6.3×10^{13}	0.0	1.104×10^5	1.0×10^{14}	0.0	2.82×10^4
28.	$N_2O + H \leftrightarrow + N_2 + OH$	6.7×10^{13}	0.0	1.52×10^4	2.5×10^{12}	0.0	7.8×10^4
29.	$NO_2 + M \leftrightarrow O + NO + M$	1.1×10^{16}	0.0	6.6×10^4	1.1×10^{15}	0.0	1.88×10^3
30.	$O_2 + N \leftrightarrow O + NO$	6.4×10^9	1.0	6.3×10^3	1.5×10^9	1.0	3.9×10^4
31.	$NO_2 + H \leftrightarrow OH + NO$	3.5×10^{14}	0.0	1.48×10^3	2.0×10^{11}	0.5	3.1×10^4
32.	$NO + HO_2 \leftrightarrow OH + NO_2$	3.0×10^{12}	0.0	2.4×10^3	1.0×10^{11}	0.5	1.2×10^4
33.	$N_2O + O \leftrightarrow NO + NO$	1.0×10^{14}	0.0	2.82×10^4	1.30×10^{12}	0.0	6.420×10^4
34.	$N_2O + M \leftrightarrow N_2 + O + M$	5.0×10^{14}	0.0	5.8×10^4	1.40×10^{12}	0.0	2.08×10^4
35.	$O + N_2 \leftrightarrow NO + N$	7.60×10^{13}	0.0	7.60×10^4	1.60×10^{13}	0.0	0.00
36.	$O + NO_2 \leftrightarrow O_2 + NO$	1.0×10^{13}	0.0	6.0×10^2	1.70×10^{12}	0.0	4.680×10^4
37.	$N + OH \leftrightarrow H + NO$	4.5×10^{13}	0.0	0.00	1.70×10^{14}	0.0	4.90×10^4
38.	$N + O_3 \leftrightarrow NO + O_2$	1.2×10^{12}	0.0	2.40×10^3	-	-	-
39.	$NO + NO_3 \leftrightarrow NO_2 + NO_2$	4.1×10^{14}	0.0	9.62×10^2	3.90×10^{11}	0.0	2.400×10^4
40.	$NO + M \leftrightarrow N + O + M$	4.0×10^{20}	1.5	1.51×10^5	6.40×10^{16}	0.5	0.00
41.	$OH + NO + M \leftrightarrow HNO_2 + M$	8.0×10^{15}	0.0	1.0×10^3	5.10×10^{17}	1.0	5.000×10^4
42.	$OH + HNO_2 \leftrightarrow H_2O + NO_2$	1.5×10^{12}	0.0	5.60×10^1	8.40×10^{11}	0.0	4.227×10^4
43.	$HNO_2 + O \leftrightarrow OH + NO_2$	6.0×10^{11}	0.0	4.0×10^3	-	-	-
44.	$HNO_2 + H \leftrightarrow H_2 + NO_2$	4.9×10^{11}	0.0	3.00×10^3	2.40×10^{13}	0.0	2.90×10^4
45.	$O + HNO_2 \leftrightarrow HNO + O_2$	3.0×10^{12}	0.0	1.60×10^4	-	-	-
46.	$OH + NO_2 + M \leftrightarrow HNO_3 + M$	5.0×10^{17}	0.0	0.0	1.6×10^{15}	0.0	3.08×10^4
47.	$HNO_3 + O \leftrightarrow OH + NO_3$	6.0×10^{11}	0.0	8.0×10^3	-	-	-
48.	$O + HNO_3 \leftrightarrow O_2 + HNO_2$	6.0×10^{12}	0.0	1.6×10^4	-	-	-
49.	$HNO + M \leftrightarrow H + NO + M$	3.0×10^{16}	0.0	4.9×10^4	5.4×10^{15}		3.0×10^2
50.	$NO_2 + O + M \leftrightarrow NO_3 + M$	1.1×10^{19}	0.0	0.0	2.5×10^9		0.0
51.	$NO_3 + H \leftrightarrow OH + NO_2$	3.5×10^{14}	0.0	1.5×10^3	-	-	-
52.	$HNO + O \leftrightarrow OH + NO$	4.9×10^{11}	0.5	2.0×10^3	-	-	-
53.	$NO_2 + N \leftrightarrow NO + NO$	6.3×10^{14}	0.0	0.0	9.0×10^9		7.839×10^4
54.	$NO_2 + N \leftrightarrow N_2O + O$	4.7×10^{12}	0.0	0.0	-	-	-
55.	$NO_2 + N \leftrightarrow N_2 + O_2$	1.1×10^{12}	0.0	0.0	-	-	-
56.	$NO_2 + N \leftrightarrow N_2 + 2O$	1.4×10^{12}	0.0	0.0	-	-	-
57.	$NO + NO + O_2 \leftrightarrow NO_2 + NO_2$	1.2×10^9	0.0	1.06×10^3	2.00×10^{12}	0.0	2.70×10^4
58.	$NO_3 + NO_3 \leftrightarrow 2NO_2 + O_2$	6.1×10^{12}	0.0	6.0×10^3	-	-	-
59.	$HNO + H \leftrightarrow H_2 + NO$	4.8×10^{12}	0.0	0.0	1.4×10^{13}	0.0	5.526×10^4
60.	$HNO + OH \leftrightarrow NO + H_2O$	6.3×10^{13}	0.0	0.0	2.40×10^6	0.0	5.0×10^3
61.	$HNO_3 + OH \leftrightarrow H_2O + NO_3$	8.0×10^{10}	0.0	0.0	1.40×10^{-2}	0.0	2.237×10^4
62.	$NH_3 + M \leftrightarrow H + NH_2$	9.2×10^{15}	0.0	8.48×10^4	-	-	-
63.	$NH_3 + H \leftrightarrow H_2 + NH_2$	1.0×10^{12}	0.0	6.28×10^3	-	-	-
64.	$NH_3 + O \leftrightarrow NH_2 + OH$	1.5×10^{12}	0.0	6.04×10^3	-	-	-
65.	$NH_3 + OH \leftrightarrow H_2O + NH_2$	2.0×10^{13}	0.0	3.006×10^3	-	-	-
66.	$NH_2 + OH \leftrightarrow H_2O + NH$	3.0×10^{10}	0.679	1.3×10^3	-	-	-
67.	$NH_2 + NH_2 \leftrightarrow NH_3 + NH$	4.0×10^{10}	0.0	5.60×10^3	-	-	-
68.	$N_2H_4 + H \leftrightarrow H_2 + N_2H_3$	1.3×10^{13}	0.0	5.520	-	-	-
69.	$N_2H_4 + M \leftrightarrow NH_2 + NH_2 + M$	4.0×10^{15}	0.0	4.12×10^4	1.0×10^{16}	0.0	0.0

70.	$N_2H_4 + O \leftrightarrow H_2O + N_2H_2$	7.1×10^{13}	0.0	1.20×10^{3}			
71.	$N_2H_4 + NH_2 \leftrightarrow NH_3 + N_2H_3$	1.0×10^{13}	0.0	5.6×10^{3}	3.3×10^{6}	0.0	0.0
72.	$N_2O_4 + M \leftrightarrow NO_2 + NO_2 + M$	1.8×10^{17}	0.0	1.11×10^{4}	1.7×10^{13}	0.0	1.72×10^{3}
73.	$N_2O_5 + M \leftrightarrow NO_2 + NO_3 + M$	1.3×10^{19}	0.0	1.944×10^{4}	2.0×10^{17}	0.0	9.62×10^{2}

bulk solution temperature. This will lead to a decrease in the maximum collapse temperature which will lead to decrease the formation of primary radicals. In addition, the reaction kinetics may increase with increasing bulk solution temperature. Moreover, the gas concentration, surface tension and other physical properties of the liquid can be affected by bulk liquid temperature increases which can influence the cavitation phenomena [60].

The sonochemical reaction can be carried out in different solvents depending on the nature of the solution. The maximum temperature obtained during cavitation bubble collapse is heavily relies on the vapor pressure of the solvent. If the collapse temperature influences a sonochemical reaction, then a low vapor pressure solvent is preferable. For instance, high collapse temperature is needed to pyrolyze volatile solutes. Moreover, the solubility of a solute is also an important parameter that needs to be considered [65]. If the solute does not dissolve in water, then the organic solvent is suitable for sonochemical reactions. $R^{\bullet}$, $H^{\bullet}$, $Cl^{\bullet}$ radicals are formed if the sonication is carried out in a non-aqueous solution such as CCl_4, $CHCl_3$, benzene, dodecane. Henglein and Fischer have experienced the formation of several radicals by sonolysis of aqueous chloroform as mentioned in equation (34). Suslick and Flint [66] have observed that sonolysis of dodecane can produce carbon radicals (e.g., C_2*)

$$CHCl_3 \rightarrow CCl_2^{\bullet}, CCl_3^{\bullet}, CHCl^{\bullet}, H^{\bullet}, Cl^{\bullet} \qquad (34)\ [66]$$

1.4 Sonoelectrochemistry

Electrochemistry is the study of reactions which occurs due to an electrochemical potential applied to a chemical system. The principal mechanism involved in electrochemistry is the transfer of electrons between the electrode and the electrolyte solution. Sonoelectrochemistry is the pairing of ultrasound energy with an electrochemical system [10]. Ultrasound was first introduced in water electrolysis in the 1930s using a platinum electrode, which took place at lower voltages and faster rates than silent conditions [67]. The effect of ultrasound irradiation is not only upon the heterogeneous system involving the electrode and the electrolyte, but also the homogeneous system that takes place in the bulk solution may experience the extreme condition produced by acoustic cavitation. The sonochemical effect by acoustic cavitation may give rise to a new reaction mechanism into the solution [10].

Ultrasound irradiation in electrochemistry can impart some particular advantages such as:

1. Degassing of the electrode surface.
2. Disruption of the diffusion layer.
3. Enhanced mass transfer of ions through the double layer.
4. Activation and cleaning of the electrode surface [10].

Many ultrasonic factors affect electrochemistry. Acoustic streaming, turbulent flow, microjets, shock waves as well as chemical effects are the major influencing factors on electrochemistry [10]. Acoustic streaming can take place in three different regions: a) in the bulk solution, b) on the reactor walls and c) at the boundary layer. The power of acoustic streaming is directly proportional to the intensity of ultrasound, the surface area of the ultrasonic emitting device and the attenuation coefficient of the medium. It is inversely proportional to the bulk solution viscosity and the speed of sound [68]. The major effect caused by acoustic streaming is the enhancement of the movement of the solution, reducing the diffusion boundary layer and enhancing the mass transfer of electroactive compounds to the electrode surface [11].

Turbulent flow is caused by the movement of the acoustic cavitational bubbles. The intensity of the turbulence is higher close to the emitting surface and decrease gradually with increasing distance. It enhances the mass transport process within the solution and the electrode surface similar to acoustic streaming [69].

Collapsing of acoustic bubbles on a solid surface leads to the formation of microjets being directed towards the surface of the solid material at speeds of up to 200 $ms^{-1.}$ Microstreaming is also caused by the bubble close to the surface [70]. If the surface is an electrode, the combined effect of the microjet and microstreaming promotes mass transport to the electrode surface. Moreover, electrode cleaning and surface activation can also be imparted by microjets that prevent fouling of the electrode surface and enhance the electrodeposition process [60]. Another mechanical effect that ensues from acoustic cavitation is shock waves generated at the end of the violent collapse of bubbles. It causes erosion of the electrode surface leading to increases in the current [11]. Besides the mechanical effect caused by acoustic cavitation, there will also be sonochemical effects in electrochemistry. Highly reactive radicals such as; HO•, HO_2•, and O• are formed due to acoustic cavitation in aqueous media [10]. In several electrochemical processes such as; electrodeposition of lead dioxide on glassy carbon, the sonochemical effect was studied related to the generation of

radicals from the sonolysis of electrolytes. However, sonochemical effects in sonoelectrochemistry were not studied as widely as the mechanical effects discussed above [71].

In water electrolysis, the cell voltage is a crucial factor that represents energy consumption. The thermodynamic decomposition voltage of water electrolysis is 1.23V, and the theoretical energy consumption for producing 1 m^3 of hydrogen is 2.94 kWh/m^3H_2 calculated according to the equation (35) [49].

$$Wt = UIt = UQ = 1.23 \times \left(2 \times \frac{1000}{22.4} \times 96485 \times \frac{1}{1000} \times \frac{1}{3600}\right) = 2.94\ kWh/m^3H_2 \qquad (35)[49]$$

Here, U = Decomposition voltage of water, I = current. Based on Faraday´s law, the electric quantity (Q) required for producing 1 mol of hydrogen is 2F. However, gas evolution in a cell does not occur until 1.65-1.7 V. Therefore, the practical energy consumption is around 4.78 kWh/m^3H_2. The energy efficiency (η_e) of hydrogen production through water electrolysis is 61.5% [49].

The practical cell voltage is expressed in equation (36), where E_a is anode potential for the oxygen evolution reaction, E_c is cathode potential for hydrogen evolution reaction, i current density, $\sum R$ total ohmic resistance, U^θ is theoretical decomposition voltage, η_a anode over potential, and η_c cathode over potential [49].

$$U_{cell} = Ea - Ec + i \times \sum R = U^\theta + |\eta a| + |\eta c| + i \times \sum R \qquad (36)\ [49]$$

Based on the equation (36), the total cell voltage is influenced by the reaction theoretical decomposition voltage, overpotential and ohmic voltage drop. Therefore, hydrogen production by water electrolysis should focus on reducing those factors. The theoretical decomposition voltage is a constant at specific temperatures, and it can be reduced by elevating the electrolytic temperature [49].

For increasing the rate of water electrolysis, the access overpotentials of η_a, η_c are essential to overcome the energy barrier. Electrode materials and the effective electrode surface area play a crucial role on reaction overpotential. During electrolysis, many bubbles absorbed on the electrode surface act as an electric shield, which reduces the effective surface area of the electrode. As a consequence, the current distribution of the electrode surface is disturbed. The increasing current density on the electrode surface increases reaction overpotential, which leads to high cell voltage and energy consumption. Another critical factor that leads to high energy consumption in water electrolysis is the ohmic voltage drop [49]. The total ohmic resistance of water electrolysis is expressed in equation (37).

$$\sum R = R_e + R_m + R_b + R_c \quad (37)\ [49]$$

Where R_e electrolyte resistance, R_m membrane resistance, R_b bubble resistance and R_c circuit resistance. The R_m and R_c are constant in an electrolytic cell, which can be minimized by optimizing the wire connection and production process of the membrane. The dispersion of bubbles in the electrolyte decreases the conductivity and increases R_e . In addition, the bubble coverage on the electrode surface act as a shield for the electric field, which leads to a high bubble resistance R_b [49].

There is experimental evidences that the reaction overpotential and ohmic voltage are reduced significantly by ultrasonication. Zadeh [72] has investigated the effect of ultrasound for hydrogen production through alkaline water electrolysis. He has used both 0.1 M NaOH and KOH solution and has found that ultrasound reduces the decomposition potential as well as the reaction overpotential. For example, in 0.1 M KOH solution, the decomposition overpotential is 2.52 V. Using ultrasound at 20kHz, the decomposition potential is reduced to 2.14 V. In addition, the overpotential without ultrasound for the same solution is 1.30 V, whereas with ultrasound it is reduced to 0.92 V [72].

1.5 Measuring techniques of radicals formed by cavitation

Formation of OH radicals through acoustic cavitation was first observed by ESR (Electron Spin Resonance) spectra of spin-trapped radicals from aqueous solution DMPO (5,5-Dimethyl-1-Pyrroline N-oxide) saturated with argon[73]. They also have observed the formation of hydrogen radicals (H•) in addition to OH radicals. In addition, the formation of OH and H radicals was confirmed by adding OH and H scavengers such as methanol, ethanol, and acetone where the decrease of ESR signals was witnessed (Figure 8) [73].

When the generation of radicals are high, the Fricke (Fe^{2+}/Fe^{3+}) method is proved to be appropriate; however, in general, the yields are low [60]. The more direct evidence of OH radicals formation has been carried out by terephthalate dosimetry. Terephthalic acid generates terephthalate anions in an aqueous alkaline solution. When OH radicals react with terephthalate ions, they produce highly fluorescent 2-hydroxyterephthalate ions [74]. The fluorescence intensity can be used to quantify the number of hydroxyl radicals [60]. Luminol (5-amino-1,2,3,4-tetrahydrophthalazine-1,4-dione) is oxidized by OH radicals that results in chemiluminescence, which can be used to quantify the amount of OH radicals formed by acoustic cavitation. Potassium iodide dosimetry can

661 do a simpler method for the quantitation of oxidants produced through acoustic cavitation
662 according to reaction (38). This method is also known as Weissler method [75].

663 $$2OH\bullet + 2I^- \rightarrow 2OH^- + I_2 \qquad (38)\ [75]$$

664

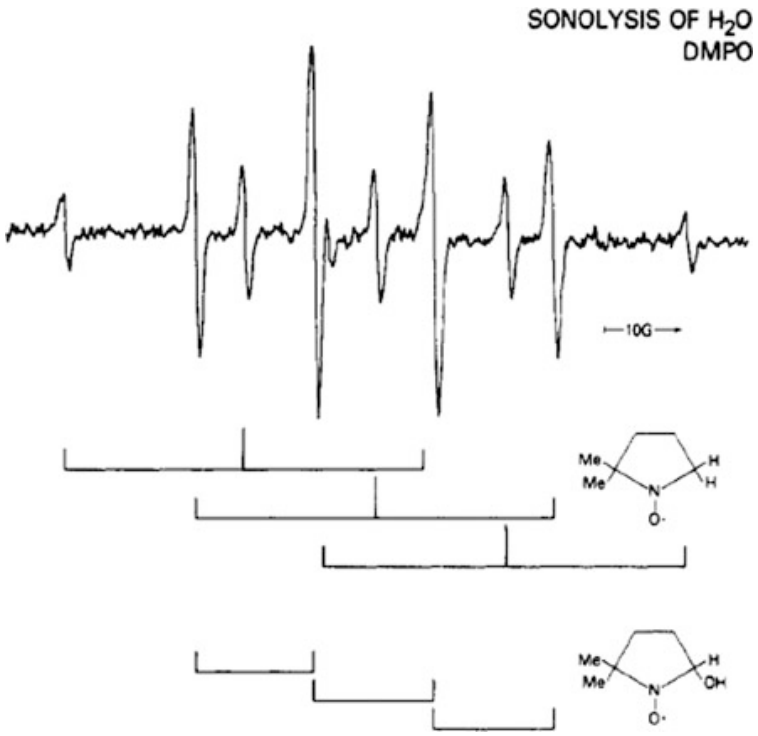

665

666 *Figure 8: ESR spectrum of Ar-saturated DMPO solution (25 mM) with 50 kHz ultrasound irradiation.*
667 *The spectrum shows the creation of OH and H radicals by sonolysis of water* [73] .

668 The excess I^- present in the solutions reacts with I_2 to produce I_3^-, and its absorption at 353 nm can
669 be utilized to quantify the amount of iodine and hence the number of hydroxyl radicals formed. A
670 standard KI concentration of 0.1M is normally used for this kind of experiment. The typical
671 average concentration of oxidants generated by acoustic cavitation per hour is around 10 µM [76].

672 *Table 5: Summary of the measuring techniques of radicals formed by acoustic cavitation.*

No.	Measuring parameter	Measuring technique	Ref.
1	Hydrogen peroxide	**Hydrogen peroxide test kit, Model HYP-1, Hach** Titration of the dye solution against sodium thiosulfate in the presence of ammonium molybdate and an acid catalyst	[77], [78]

2	Hydroxyl radicals ($OH^{\bullet}$)	**Terephthalic acid (TA) dosimetry:** Terephthalic acid solution of 0.002 mol/l was sonicated, and then fluorescence measurement was performed using LS-50 luminescence spectrometer.	[79]–[81]
3	Hydroxyl radicals ($OH^{\bullet}$)	**Salicylic acid dosimetry**: 500 μM salicylic acid was subjected to sonication in different ultrasonic frequency and the concentration of salicylic acid and hydroxylated products were quantified by HPLC.	[82], [83]
4	Hydroxyl radicals ($OH^{\bullet}$)	**Coumarin fluorometry:** Coumarin solution of 0.1 mM was exposed to ultrasonic irradiation, and then the chemo-fluorescent diagnosis was carried out using with UV-visible spectroscopy and fluorescent spectroscopy.	[84]
5	Hydroxyl radicals ($OH^{\bullet}$)	**Methyl Orange dosimetry:** Methyl orange solution was sonicated with fixed frequency and power at different times. Then the concentration of the sonicated solution was measured by US-vis spectrophotometer	[85]–[87]
6	Hydrogen Peroxide	**KI dosimetry:** 0.1 M KI was dissolved in water and the absorbance of I_3^- was measured at 304 nm by UV spectrometer.	[81], [86], [88], [89]
7	Hydrogen peroxide and nitrous acid	US-visible spectroscopy	[90], [91]
8	Hydroxyl radicals ($OH^{\bullet}$) and H_2O_2	**Fricke dosimetry:** $FeSO_4$ $(NH_4)_2SO_4.6H_2O$ of 1 mM, 96% H_2SO_4 of 0.4 M, and NaCl of 1 mM were dissolved in water. UV spectrometer was used to measure the absorbance of Fe^{3+} at 304 nm.	[81]

2. Sonochemical production of hydrogen

Use of ultrasound in clean hydrogen production could be a promising method if water is used as hydrogen source. In addition, hydrogen production using ultrasound from catalysis [92], photocatalysis [93], digestion sludge [94] and anaerobic fermentation [95] of wastewater have been proved to be efficient compared to each isolated method. Harada [54] has studied the isolation of hydrogen from water through photocatalysis assisted by ultrasound using an alternating irradiation method. In this method, ultrasound and light are irradiated in turn. Sonophotocatalysis was also used in isolating hydrogen from sea water.

Hydrogen production by water sonolysis does not occur from the interaction between the acoustic waves and the water, but it evolves from the acoustic cavitation. It is well established that H_2 and H_2O_2 are the main products with ~1.25 ratio (H_2:H_2O_2) when pure water undergoes sonication [9] . The rapid collapse of microbubbles due to cavitation produces localized enormous temperature and pressure that leads to combustion-chemistry inside the bubble [96]. As a result, highly reactive species such as $OH\bullet$, $H\bullet$, O, $HO_2\bullet$, and H_2O_2 are produced [97]. The diffusion of radicals begins

688 inside the bubble into and is ejected into the surrounding liquid [98]. Hydrogen is one of the most
689 occurring products in water sonolysis. It is produced at the rate of 10-15 μMmin^{-}1 [99], [100]. The
690 amount is much higher than that obtained by photocatalysis (~0.035 μMmin^{-}1 [101]).
691 The mechanism of hydrogen production through acoustic cavitation is under discussion till date
692 [9]. The major part of the hydrogen is produced in the gas phase of the bubble and diffuse out to
693 the surrounding solution [102], [103]. Some researchers have proposed that hydrogen is produced
694 only at the bubble wall through recombination of hydrogen radicals ($H\bullet + H\bullet \leftrightarrow H_2$) [104], [105].
695 Merouani et al. [64] has extensively studied the mechanism of hydrogen production by sonolysis.
696 A comprehensive numerical study was undertaken in an attempt to explain the mechanisms of
697 sonochemical hydrogen production. Chemical reactions occurring inside a bubble at different
698 conditions due to ultrasonic cavitation was performed by computer simulation. To study the
699 internal bubble chemistry, kinetics of 25 reversible chemical reactions were proposed [64]. The
700 production of hydrogen gas as well as other products such as O_2, $HO_2\bullet$, O, H_2O_2, $OH\bullet$ and $H\bullet$ was
701 observed through the numerical simulation. Hydrogen was the main products in all cases. Based
702 on simulation results, it was proposed that the main source of hydrogen production by water
703 sonolysis is the gas phase of the bubbles according to the reaction (39). Almost 99.9 % [106] of
704 the hydrogen is produced from the gas phase recombination reaction. However, the recombination
705 reaction (40) occurring at the shell of the bubble plays a minor role in hydrogen production.

706 $$H\bullet + OH\bullet \leftrightarrow H_2 + O \qquad (39)$$

707 $$H\bullet + H\bullet \leftrightarrow H_2 \qquad (40)\ [106]$$

708 Henglein [107] has investigated the sonolysis of methane in aqueous solution and has produced
709 significant amount of hydrogen gas along with oxidation products such as ethane, ethylene, C_3-C_4
710 hydrocarbons and carbon monoxide. It is seen that the production of H_2O_2, one major product of
711 water sonolysis decreased drastically. These indicates the strong interaction of methane with water
712 sonolysis. Methane reacts with both $H\bullet$ and $OH\bullet$ radicals generating from water sonolysis
713 according to equation (41) and (42).

714 $$CH_4 + OH\bullet \rightarrow CH_3 + H_2O \qquad (41)$$

715 $$CH_4 + H\bullet \rightarrow CH_3 + H_2 \qquad (42)\ [107]$$

716 The reduction of hydrogen peroxide formation is understood based on the equation (41) and (42).
717 The recombination reaction of $H\bullet$ and $OH\bullet$ caused by water sonolysis saturated with pure argon

718 limits the formation of hydrogen gas and hydrogen peroxide. Methane helps to suppressed the
719 recombination reaction, thus increases in H_2 production are observed by reducing H_2O_2. In addition
720 to this, methane can be thermally decomposed producing H•, which contributes to higher H_2 yield
721 according to equation (43) [107].

722 $$CH4 \rightarrow CH_3 \bullet + H\bullet \qquad (43)\ [107]$$

723 Wang et al. [108] has studied the effect of a Au/TiO_2 catalyst in the sonochemical production of
724 hydrogen. They have found that with the presence of Au/TiO_2, the rate of hydrogen evolution
725 increases significantly in the sonolysis of water and methanol solution. Product analysis and
726 isotope evidence indicate that hydrogen is evolved by three pathways from methanol/water
727 solution: (1) recombination of two hydrogen atom produced by sonolysis of water molecules, (2)
728 H-abstraction from methanol by H•, and (3) thermal reforming of methanol. Experimental results
729 showed that nearly half of the hydrogen is produced from water molecules although the addition
730 of methanol increases the hydrogen evolution in 12-fold. They also have studied the hydrogen
731 evolution with bare TiO_2 and in the absence of a catalyst. The compositions of produced hydrogen
732 gas were similar in both cases. However, the evolution rate was much slower. That indicates the
733 influence of Au nanoparticles on the TiO_2 surface to catalyze the water sonolysis and methanol
734 reforming effectively [108].
735 Several factors influences the sonochemical production of hydrogen. These includes ultrasonic
736 frequency, dissolved gas, ultrasonic power and liquid temperature.
737 **2.1 Effect of ultrasonic frequency**
738 The most dominant factor in acoustic cavitation induced sonolysis of the aqueous solution is the
739 applied frequency [106]. Generally, in sonochemistry, ultrasonic frequencies are used in the range
740 of 20 kHz to ~1 MHz. The optimum ultrasonic frequency for sonochemistry has been reported to
741 be around 355 kHz considering the rate of oxidant production by bubbles. On the other hand, the
742 most widely used ultrasound frequency for sonochemistry is 20 kHz [109]. Merouani et al. [106]
743 al has studied the effect of ultrasonic frequency in the range of 20-1140 kHz through numerical
744 simulation for hydrogen production inside the collapsing argon and air bubble. The acoustic
745 intensity was 1 W cm^{-2} and the bulk liquid temperature was 20°C [106].

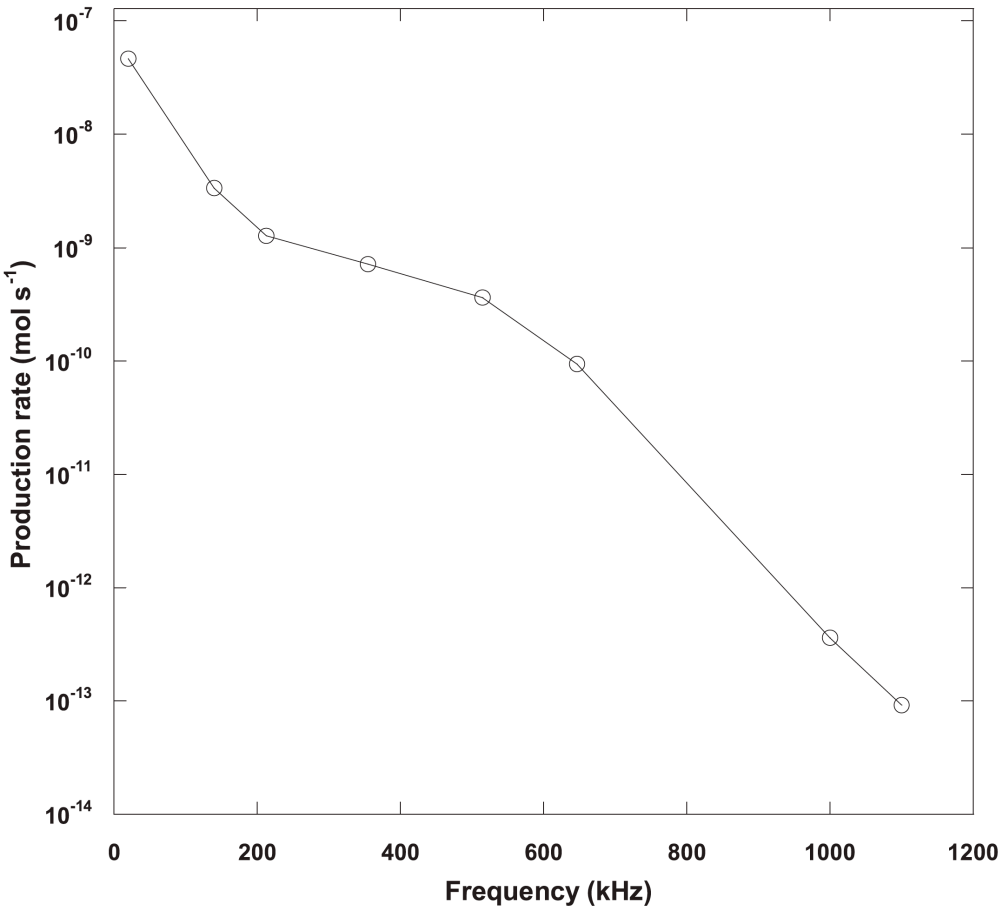

Figure 9: Production rate of hydrogen from a single bubble as a function of ultrasonic frequency. The vertical axis is in logarithmic scale [106].

As can be seen from Figure 9, the rate of production of hydrogen decreases with the increase in ultrasonic frequency significantly in the range of 20-1100 kHz. The frequency affects the maximum bubble temperature, pressure, collapse times and the quantity of water vapor trapped at the collapse. The cavitation bubbles get more time to expand with a smaller frequency, which leads to a more substantial expansion and compression ratio. This phenomenon results in higher temperatures and pressures, which accelerates the dissociation of trapped water vapor into radicals. The higher the concentration of H• and OH• radicals inside the bubble, the higher the production of hydrogen because of the recombination reactions (39). On the other hand, the reaction system inside the bubble does not get enough time to evolve at high frequency. Therefore the reactants are converted into free radicals due to the shorter collapse time. It is expected that the production

760 rate of hydrogen is higher at a lower frequency (20kHz) and gradually decrease with increasing
761 frequency [106].
762 The number and size of active cavitation bubbles are also influenced by ultrasonic frequency [106].
763 It is predicted that with the increase in the ultrasound frequency, the amount of active cavitation
764 bubbles increases [110]. The experimental measurement of hydrogen production showed that the
765 yield of hydrogen at 300 kHz is in the rate of 0.83 μM min^{-1} [111] whereas at 1000 kHz the yield
766 is at the rate of 0.42-0.68 μM min^{-1} [112]. This demonstrate that among the two factors; the number
767 of active bubbles and the single-bubble yield, the single bubble event is the dominant factor in the
768 overall production of hydrogen by water sonolysis [106].
769 **2.2 Effect of ultrasonic intensity**
770 The production of hydrogen increases with increasing the ultrasonic intensity [106]; however, the
771 improved effect of the ultrasonic intensity is more apparent at higher frequencies. For a liquid
772 temperature of 20°C, the effect of ultrasonic intensity (Figure 10) on the hydrogen production rate
773 inside an argon bubble was studied by Merouani et al. [106]. The collapsing bubbles formed by
774 acoustic cavitation can be considered as microreactors, where high temperature and pressure
775 chemical reactions occur. Hydrogen is the product of one of the chemical reactions occurring
776 inside the bubble through the recombination of H• and OH•. Therefore, the production rate will
777 depend on the amount of radicals available in the gas phase. The radical production inside the
778 bubble is controlled by three factors; the amount of water vapor trapped inside the bubble, bubble
779 temperature and collapse time. The expansion and compression ratio of bubbles increases with
780 increasing acoustic intensity. Therefore, higher bubble temperatures are achieved at higher
781 compression ratios. In addition, the amount of water vapor trapped inside the collapsing bubble is
782 higher with a higher expansion ratio. As a result, the increase of both the collapse temperature and
783 amount of trapped water due to increasing ultrasonic intensity accelerates the formation of free
784 radicals through the dissociation of water vapor inside the bubble. Moreover, the bubble collapse
785 time increases with the increase in acoustic intensity. The chemical reactions occurring inside the
786 bubble at a high intensity experience more time to evolve and convert water vapor into free
787 radicals. As a consequence, higher acoustic intensities will result in elevated sonochemical effects
788 inside a bubble promoting higher hydrogen production rate [106].

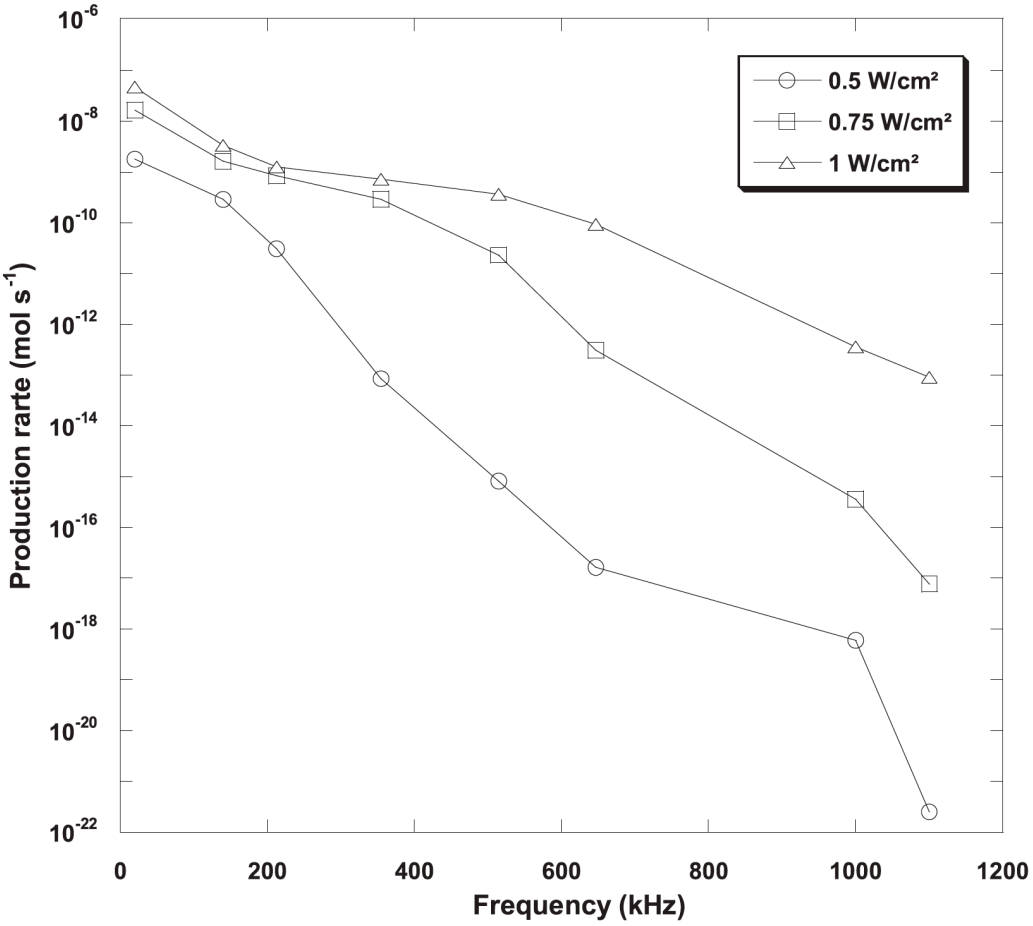

Figure 10: Production rate of hydrogen from a single bubble as a function of ultrasonic frequency for various acoustic intensities [106].

Venault [113] has experimentally demonstrated the production of hydrogen in different acoustic intensities. When argon saturated water was irradiated with ultrasound at 20 kHz frequency and 0.6 W cm^{-2} intensity, the production rate of hydrogen was 0.8 μM min^{-1}. The rate increased to 2.1 and 5 μM min^{-1} with the increased acoustic intensity of 1.1 and 2.5 W cm^{-2}, respectively [106]. Nevertheless, these yields are in a multibubble system known as a cavitation field. The effect of ultrasonic intensity cannot be elucidated based on the single bubble yield alone but also by the number of active bubbles. Considering the number of active bubbles, it was reported that the hydrogen production increased with increasing acoustic intensity [109], [114].

2.3 Effect of the nature of the solution

The nature of dissolved gas has a controversial effect on the sonochemical activity [115]. Various experimental reports demonstrate that due to a higher polytrophic ratio, argon provides more sonochemical activity than other polyatomic gases, which provide higher bubble temperature at

collapse [116]–[118]. A few other studies [119]–[121] demonstrate that polyatomic gases (i.e. oxygen) through self-decomposition can compensate for oxygen-bubble temperature, which yield more sonochemical activity compared to argon. Merouani et al. [106] have performed numerical simulations of sonochemical reactions for two saturating gases (Ar and air) at different acoustic frequencies with a constant acoustic intensity and liquid temperature of 1 W cm^{-2} and 20°C (Figure 11). With increasing frequency, the production rate of hydrogen decreases for both argon and air saturated aqueous solution. Argon saturated solutions favors more production of hydrogen during bubble collapse than air saturation, and the beneficial effect of argon becomes more phenomenal at higher acoustic frequencies (>213 kHz). However, most of the bubble content at 20 kHz is water vapor. Therefore, the saturation of water by any other gas will not affect the chemistry of the bubbles. This phenomenon leads to an identical production rate of hydrogen for both argon and air at 20 kHz.

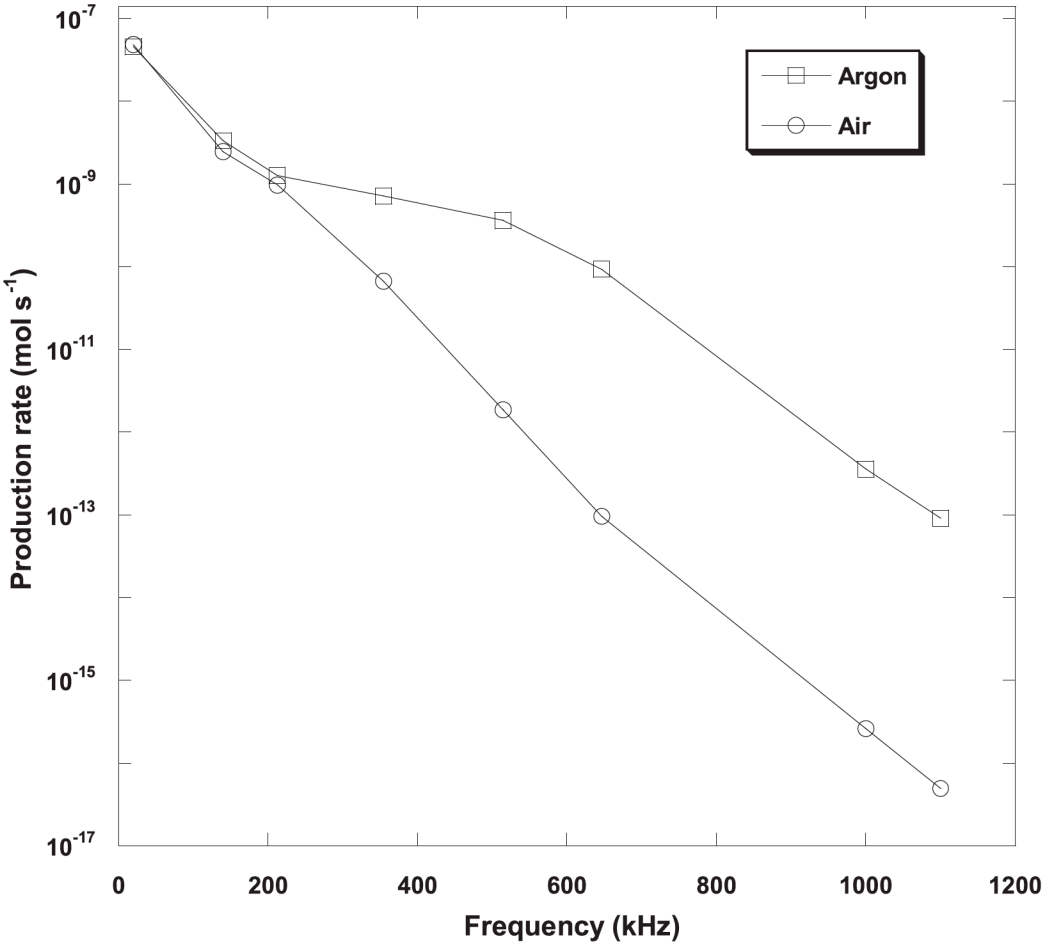

Figure 11: Hydrogen production rate from a single bubble as a function of acoustic frequency for different saturating gases [106].

The chemistry of bubbles at collapse is affected by dissolved gases through two main principles.

(1) In general, monoatomic gases have higher polytrophic indexes γ (C_p/C_v) than polyatomic gases. The higher polytrophic indexes results in elevated bubble temperature at the collapse which promotes higher sonochemical activity.

(2) Low thermal conductivities (λ) reduce the heat dissipation. Thus gases with low thermal conductivities facilitate the increase of bubble collapse temperature and consequently enhance the sonochemical activity in the bubble.

Argon has higher polytrophic ratio ($\gamma = 1.66$) and lower thermal conductivity ($\lambda = 0.018$ $Wm^{-2}K^{-1}$) than air ($\gamma = 1.41$, $\lambda = 0.026$ $Wm^{-2}K^{-1}$). Therefore, a bubble collapse in the presence of Ar favors an elevated bubble temperature [106]. Okitsu et al. [122] has experimentally demonstrated that the bubble temperature does not depend on the thermal conductivity at a higher frequency. Therefore, it is clear that argon saturated water provides highest production rate of hydrogen.

The overall hydrogen production is influenced by the single bubble yield and the number of active bubbles generated in reacting media. The generation of active bubbles is proportional to the solubility of the gases. Therefore, the higher the solubility of the gas, the higher the number of active bubbles generated. The solubility of argon ($X_{Ar} = 2.748 \times 10^{-5}$)in aqueous media is higher than the solubility of air ($X_{air} = 1.524 \times 10^{-5}$). As a result, the overall production rate of hydrogen from argon saturated aqueous solutions will be higher than air saturated solutions. Margulis and Didenko [123] have experimentally demonstrated that argon saturated water at 1000 kHz produces 61 times higher hydrogen (13.6 $\mu M\ min^{-1}$) than that of air saturated water (0.22 $\mu M\ min^{-1}$) sonolysis. Moreover, Hart et al. [100] observed that at 300 kHz the hydrogen production rate is 14 $\mu M\ min^{-1}$ in Ar atmosphere and 3.7 $\mu M\ min^{-1}$ in a nitrogen atmosphere.

2.4 Effect of liquid temperature and active bubble size

Bulk liquid temperature has a significant effect on sonochemical hydrogen production. Merouani et al. [106] has studied the effect of liquid temperature for hydrogen production from argon saturated aqueous solution. The production rate of hydrogen marginally increases with increase in temperature from 20 to 30°C and a further increase in temperature slows down the production rate (Figure 12). These results demonstrate the existence of an optimum temperature (~30°C) in sonochemical hydrogen production. This results is in line with the findings of Gong and Hart [124].

850 It is also observed that the liquid temperature variation does not affect the compression and
851 expansion ratio. However, the bubble temperature and the quantity of trapped vapor is significantly
852 affected by the rise in liquid temperature due to the increase of liquid-vapor pressure. This can
853 facilitate the formation of free radicals as they come from the water vapor. However, increasing
854 liquid temperatures can causes less violent collapse due to the decrease of the polytrophic index
855 (γ) leading to lower internal bubble temperature at collapse. Lower bubble temperature during
856 collapse lowers the formation of free radicals by decomposition of molecules. Both of these effects
857 give rise to an optimum liquid temperature for formation of radicals that leads to the maximum
858 hydrogen production [106].
859

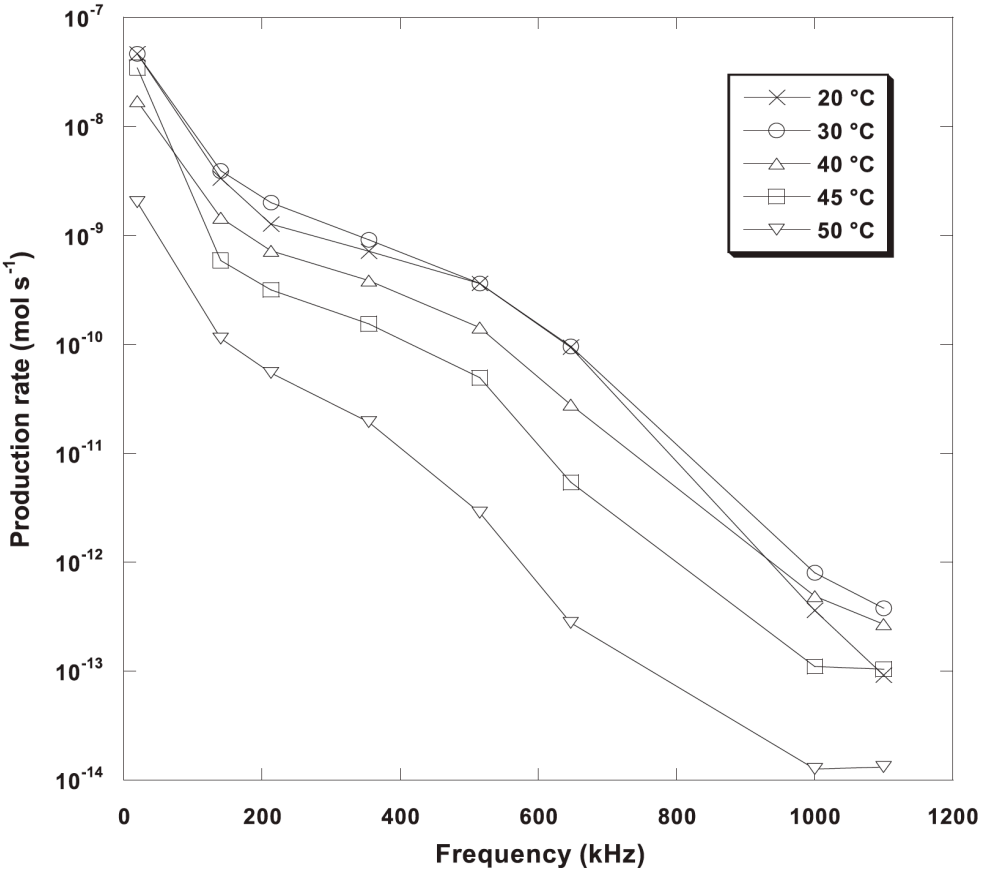

860
861 *Figure 12: Production rate of hydrogen from a single acoustic bubble as a function of acoustic frequency*
862 *for different bulk liquid temperature* [106].
863 Another influencing parameter in sonochemical production of hydrogen is the size of active
864 bubbles. Experimental studies on the effect of active bubble size is scare. Through numerical
865 simulation, Merouani et al. [4] have demonstrated that the active bubbles size includes an optimum

value where the production of hydrogen is maximum. The optimum bubble radius for hydrogen production increases with increasing acoustic intensity and decreases with increasing frequency and bulk liquid temperature. The amount of water vapor trapped in the bubble and the maximum bubble temperature at collapse are the two main factors affecting the optimum bubble size. The bubble temperature as well as the amount of trapped water vapor increase with increasing ambient bubble radius from 0.9 to 2 μm. This phenomenon promotes the production of free radicals which enhances the production of hydrogen [4].

3. Sonoelectrochemical production of hydrogen

Water electrolysis is one of the most widely used technologies for renewable hydrogen production. In an electrolytic process, hydrogen gas is produced right at the decomposition potential. The production is at the molecular level occurring on the surface of the electrode through an electrochemical reaction. At the cavity of the electrode surface, molecular hydrogen gas turns to hydrogen gas bubbles at the active cathodic sites. The gas bubbles then expand and accumulate at the surface of the electrode [72]. The total cell voltage consists of the thermodynamic decomposition voltage, the ohmic potential drop and the overpotential of the anode and cathode. Moreover, the ohmic potential drop due to the presence of gas bubbles at the electrode surface and in the solution results in high energy consumption [125]. By using an effective electrocatalyst on to the electrodes and/or by operating the electrolytic cell at a higher temperature (65-80°C), the anodic and cathodic overpotentials can be reduced [126]. The aggregation of gas bubbles at the electrode surface raise the electrical resistance of the cell [125].

The gas bubble formation is an interfacial phenomenon. The complex electrochemical interfacial phenomena influence the energy efficiency of hydrogen energy system at the three phase region of gas bubbles, electrode and electrolyte. Damaging the boundary layer of the three-phase zone enhance the mass transport of the cell [125]. Ultrasound is a powerful tool to overcome the limitations of water electrolysis for hydrogen production through

- Cleaning and activation of surfaces.
- Increasing mass transport in the bulk solution and near the surfaces.
- Alternating reaction schemes caused by sonochemical effects [49], [127].

Walton et al. [128] have studied the effect of ultrasound on hydrogen evolution from 1 M H_2SO_4 at a platinized platinum electrode with 38 kHz ultrasonic frequency. It was observed that in the presence of ultrasound there is an increase of current of 2.1 fold at the lower limit of the sweep

compared to unsonicated condition. The reduction of the proton at platinized platinum is a reversible reaction. The availability of the proton at the electrode does not improve the current caused by the enhanced diffusion. Instead, the dominant effect in hydrogen evolution is the removal of hydrogen from the electrode surface [128]. From Table 6, it can be seen that ultrasound can increase hydrogen production efficiency by 10% for 0.1M KOH solution.

Table 6: Energy consumption and efficiency of hydrogen production via various water electrolysis of an aqueous different solution

Technology	Theoretical energy consumption (kWh/m^3H_2)	Practical energy consumption (kWh/m^3H_2)	Efficiency %	Reference
Conventional Alkaline Electrolysis	2.94	3.52	83.67	[129]
Sea water	2.94	5.03	58.57	[129]
Brine electrolysis	2.94	5.33	53.25	[129]
0.1M KOH	2.94	6.3	48.81	[72]
0.1M KOH with ultrasound (20 kHz)	2.94	5.12	57.48	[72]

3.1 Solution type and concentration effect

Ultrasound-assisted water electrolysis for hydrogen production was first carried out by Cataldo (1992) [130]. The effect of ultrasound was studied (30 kHz and 1-2 Wcm^{-2}) on the yield of gases from a saturated aqueous solution of NaCl (6.0 M), HCl (6.0 M) and acidified NaCl (5.0 M NaCl/1.1 M HCl) using both platinum and carbon rods as electrodes. It was found that ultrasound dramatically increases the yield of chlorine gas and marginally increase the yield of hydrogen gas. The strong degassing effect at the surface of the electrode due to the bubble fusion caused by cavitation is the most crucial reason for enhanced gas yield. The ultrasonic effect on the gas yield is more significant for chlorine than hydrogen due to its very high solubility in water (3150 ml/l of Cl vs. 19.6 ml/l of H_2) at standard pressure and 15°C. Due to sonication, the bubbles are forced to merge into large bubbles providing a smaller gas/liquid interface. In addition, due to the minimal contact time between the gas bubbles and the aqueous solution, the bubbles are pushed out from the solution at high speed. This phenomenon leaves the solution free from dissolved gases. The dispersed gas bubbles generated during electrolysis reduce the electrical conductivity of the

919 solution, which is also called the bubble effect. The drop of conductivity is directly proportional
920 to the concentration of gas bubbles dispersed into the liquid. Ultrasound enhances the diffusion of
921 the gas bubbles from the liquid, thus increase the gas yield [130].
922 The yield of hydrogen is marginally higher from acidified sodium chloride solution than saturated
923 sodium chloride solution. In addition, hydrogen yield from 22% HCl (6.0 M) is the highest among
924 all the above mentioned solutions [130]. Walton et al. [128] have studied the effect of ultrasound
925 (38 kHz) for chlorine, hydrogen and oxygen evolution at the platinized electrode. 1M H_2SO_4
926 solution was used for hydrogen evolution and 2.5 M NaCl/0.1 M HCl was used for chlorine gas
927 evolution. They proposed that, the reduction of hydrogen ions in platinized platinum electrode is
928 a reversible reaction. The availability of H^+ is such that enhanced diffusion of the proton will not
929 improve the current. The rate determining step in hydrogen evolution is the product removal from
930 the electrode surface; therefore, ultrasound plays a crucial rule in hydrogen evolution.
931 Zadeh [72] has studied the ultrasound-assisted (20 kHz) alkaline water electrolysis for hydrogen
932 production. NaOH and KOH solutions of 0.1M were used as electrolytes. It was observed that
933 hydrogen production was improved by 14% and 25%, respectively for NaOH and KOH during
934 sonication. The higher production rate of hydrogen from KOH than NaOH is due to the higher
935 conductivity of the KOH solution.
936 Li et al. [125] have studied the effect of the ultrasound (60 kHz and 50 W) for water electrolysis
937 in different electrolyte concentrations of 0.1M, 0.5M and 1.0M NaOH solution. The Linear Sweep
938 Voltammetry (LSV) curves were obtained at these concentration in order to understand the effect
939 of ultrasound for Hydrogen Evolution Reaction (HER) and Oxygen Evolution Reaction (OER).
940 Figure 13 represents the effect of ultrasound on the cell voltage, HER and OER with different
941 electrolyte concentrations. It was observed that the cell voltage, anode and cathode potential were
942 significantly decreased at higher electrolyte concentration. This was due to the decrease of the
943 resistance of the electrolyte. From the LSV curves, it is clear that ultrasound has a positive effect
944 into water electrolysis at lower electrolyte concentration [125].
945 Moreover, water electrolysis was also performed galvanostatically for 1h at different electrolyte
946 concentration presented in Figure 14 [125] showing the cell voltage differences with and without
947 ultrasound for several current densities. It is observed that, with ultrasound, the cell voltage is
948 lower than without ultrasound (Figure 14(a)). The reduction of cell voltage at same concentration

is also decreased with increasing electrolyte concentration. This is due to the enhanced mass transfer rate of the electrolyte at higher concentration.

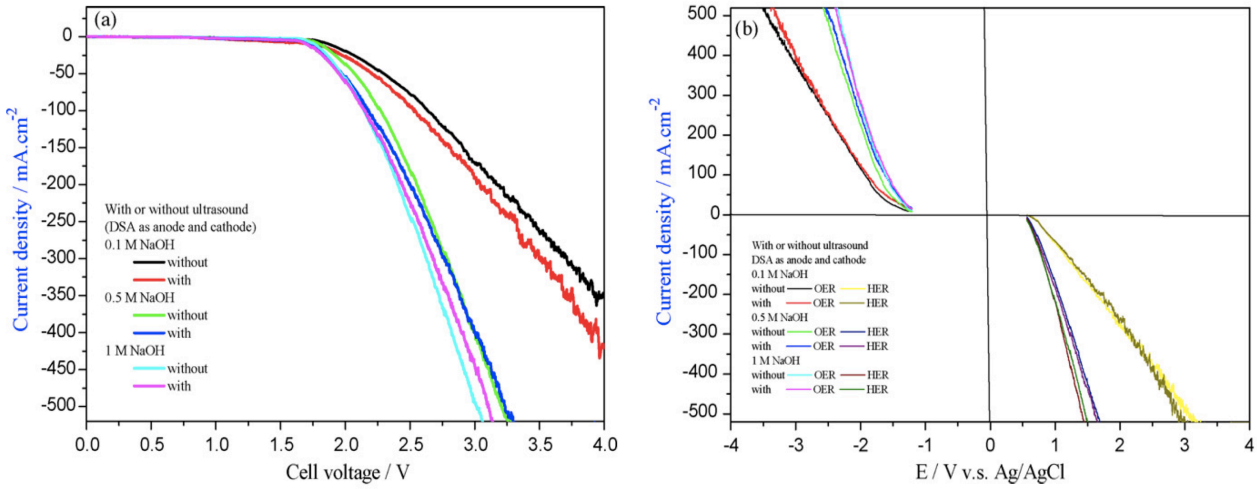

Figure 13: LSV curves of (a) the cell voltage , (b) HER and OER with and without ultrasound [125].

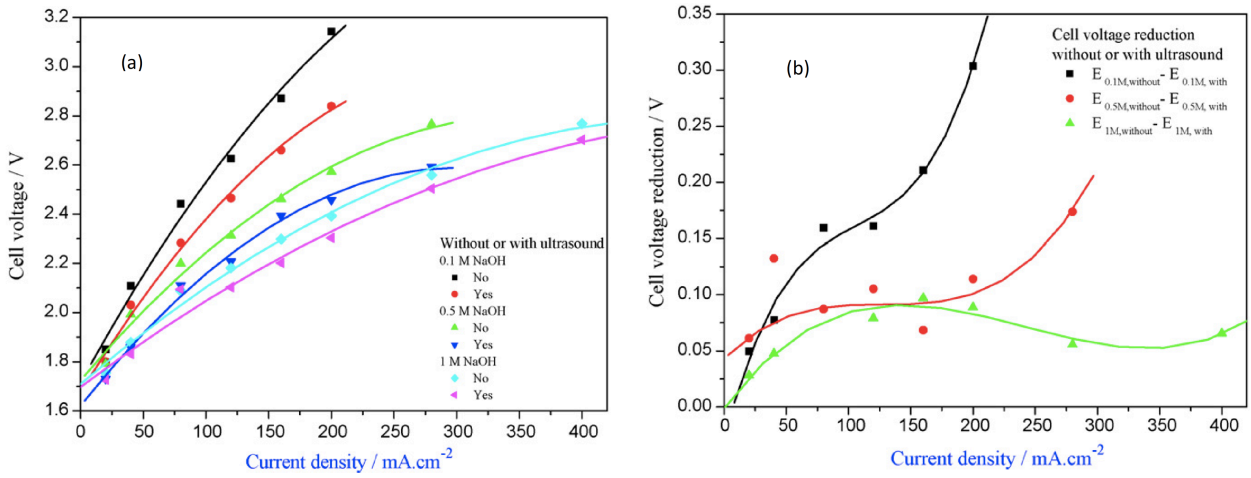

Figure 14: (a) Steady state E-I curves of water electrolysis at different NaOH concentration with and without ultrasonication, (b) Reduction of cell voltage as a function of relative current densities. (ΔE = E without- E with at the same concentration) [125].

The reduction of cell voltage at lower concentration is increased with current densities but it is almost constant at higher electrolyte concentration [125]. Without ultrasound, the efficiency of hydrogen evolution decreases with increasing electrolyte concentration. The electrolyte concentration influences the hydrogen bubble size and applied cell voltage. The bubble size becomes smaller with increasing electrolyte concentration [125], [131].

963 The efficiency of hydrogen generation without ultrasound is in the range of 60-75%. On the other
964 hand, by the presence of ultrasound, the efficiency is improved significantly, and it is in the range
965 of 80-85%. Moreover, the efficiency increases with increasing electrolyte concentration in the
966 range of 5-18%. This is due to the rapid removal of bubbles from the electrode surface by the
967 ultrasound followed by refill of the nucleation sites by new gas bubbles [125] .

968 **3.2 Current and voltage effect**

969 Li et al. [132] has investigated the effect of ultrasound (25.3 and 33.3 kHz) on the electrolysis of
970 NaOH solutions for hydrogen production. It was observed that ultrasound helps to reduce the
971 anode cell voltage. With increasing current densities, the decrease of the anode voltage was
972 insignificant. A marginal decrease of anode voltage was observed at lower current densities (20
973 mA/cm^2, 30 mA/cm^2, 40 mA/cm^2). At higher current densities (75, 150, 200 mA/cm^2), the anode
974 voltage decreased about 200-320 mV. The generated oxygen gas at the anode covered the electrode
975 surface by forming a thin film around the electrode. This leads to a higher anodic voltage.
976 Ultrasound irradiation can break down this thin film by removing the oxygen gas bubbles from the
977 anode, which leads to decrease in the anodic voltage [132].

978 Li et al [125] have observed that, ultrasound helps to reduce the cell voltage and lowering the cell
979 voltage increases the efficiency of hydrogen production. The values of cell voltage reduction at
980 0.1 M, 0.5 M and 1.0 M NaOH are about 320 mV, 100 mV and 75 mV at constant current density
981 of 200 $mAcm^{-2}$ [125]. Qian et al. [133] have stated that the bubble surface coverage is proportional
982 to the ohmic resistance. Ultrasound can easily remove the gas bubbles from the electrode surface
983 and from the bulk electrolyte in order to reduce the bubble surface coverage and the void fraction
984 of the bulk electrolyte, respectively [133].

985 Cataldo [130] has experimented with the evolution of hydrogen using carbon rod cathodes and
986 anodes with same electrolyte of 5.0M NaCl/1.1 M HCl solution at different cell voltages. Under
987 sonication, the production of hydrogen is higher when a higher cell voltage is applied (e.g. 0.00418
988 g of hydrogen at 8 V, and 0.0046 g of hydrogen at 20 V). During sonication, Cataldo [130] has
989 witnessed a clear increase in current through the cell. The percentage growth of current was
990 calculated according to the equation (44)

991 $$Z=[(I_m - I_e)I_e]100\%. \qquad (44)\ [130]$$

992 Where I_e = the steady-state current, and I_m = net increase of current through the cell under
993 sonication. At constant acoustic intensity and frequency (30 kHz and 1-2 W/cm^2) and at low

994 current density the Z was approximately 10%; however, the Z value becomes negligible at high
995 current density. When Z = 0%, an efficient degassing under sonication was observed. This means,
996 the increase of current (can be seen as depolarization or an attenuation of overpotential) during
997 sonication is not due to coalescence of bubbles and degassing. The depolarization by
998 ultrasonication is due to cavitation and ultrasonic waves. They can stir the bulk solution efficiently,
999 eliminating the contribution of the concentration gradients to the overpotential. Moreover, they
1000 allow the transfer of the ions across the electrode double layer. By increasing the acoustic intensity,
1001 it would be possible to experience a depolarizing effect also at very high current density [130].
1002 Recently Lin and Hourng [134] have studied the ultrasonic (133 kHz frequency) wave field effect
1003 on water electrolysis for hydrogen production, where alkaline KOH was used as the electrolyte.
1004 They have found that at 30 wt.% electrolyte concentration and low potential state, ultrasound
1005 enhanced the activation polarization. Electrolyte concentrations of above 30 wt.% improved the
1006 concentration polarization. Improvement of activation polarization and concentration polarization
1007 accelerated the rising of hydrogen gas bubbles during water electrolysis. At 4V electric potential,
1008 40 wt.% electrolyte concentration and with a 2 mm electrode gap, the difference of current density
1009 for water electrolysis with ultrasonic power of 225 W and without ultrasound was 240 mA/cm^2 .
1010 This allowed for a power saving of 3.25 kW as well as an economical power efficiency of 15%
1011 [134]. A summary of experimental conditions for sonoelectrochemical production of hydrogen is
1012 provided in Table 7.
1013
1014 *Table 7: Summary of sonoelectrochemical hydrogen production*

No.	Ultrasound frequency (kHz)	Ultrasound power	Electrode material	Electrolyte and concentration	Cell Voltage (V)	Current density	Reference
1	30	1-2 W/cm^2	Carbon rod and platinum leaf	6 M NaCl, 6 M HCl and 5.0 M NaCl/1.1 M HCl	8, 10, 12, 20	2.7, 6.5, 7.6 (Adm^{-2})	[130]
2	38	-	Platinum	1 M H_2SO_4	-	50 mA cm^{-2}	[128]
3	20	26 W/cm^2	Platinum sonotrode, Graphite counter electrode and SCE	0.7 M Na_2SO_4 (maintained pH at 7 by using 0.1 M NaOH)	-	-	[135]

4	60	50 W/cm^2	RuO_2 and IrO_2 plated Titanium	0.1, 0.5 and 1.0 M NaOH	-	20-400 mAcm^{-2}	[125]
5	25.3, 33.3	-	Graphite and SCE	0.4 M NaOH	-	20-200 mAcm^{-2}	[132]
6	133	225, 450, 675 and 900 W	Pure Nickel	10, 20, 30 and 40 wt. % KOH	2-4	-	[134]
7	20	-	Nickel	0.1 M of NaOH and KOH	0-30		[72]
8	42	300 W	Platinum and SCE	2M KOH	-	-	[127]

4. The need of future research

To the best of our knowledge, nobody has studied the effect of ultrasound frequency on sonoelectrochemical hydrogen production except the very preliminary investigations by Li et al. [132]. Most of the investigation was performed at single acoustic frequency. Li et al. [132] stated that higher ultrasound frequencies (25.3 kHz vs. 33.3 kHz) did not provide any significant improvement in hydrogen production. However, detailed studies need to be performed in a wide range of frequencies in order to understand their effect on sonoelectrochemical hydrogen production. In addition, the effect of ultrasound power and intensity is also required to be investigated. Different types of electrode materials are being employed to date for hydrogen production through water electrolysis.

Another area of research field that requires attention is the quantitation of the produced hydrogen. Very few studies [72], [125], [130] actually quantitated the yield of hydrogen partially. Detailed quantitation of a product is necessary to understand the effect of variable operating conditions as well as upgrading a process from laboratory scale to pilot or industrial scale. Therefore, research needs to be performed in quantitating the produced hydrogen and techno-economic analysis for an industrial application.

Moreover, to the best of our knowledge, nobody has studied the sonochemical and sonoelectrochemical production of hydrogen from a non-aqueous solution. Hence, it is necessary to investigate the feasibility of hydrogen production from various non-aqueous solutions through ultrasonication.

5. Conclusion

An enormous amount of research is being undertaken towards the development of hydrogen production technologies. Currently, the most widely used and technically developed method is the reforming of hydrocarbon. However, these methods lead to release tremendous amount of greenhouse gas into the atmosphere, which is responsible for global climate change. On the other hand, due to depletion of fossil fuels, the global awareness to reduce dependency on fossil fuel and search for alternative sources and methods for hydrogen production. Using ultrasound in hydrogen production could be a promising alternative. The primary source of hydrogen during water sonolysis is the gas phase of the bubbles. The yield of sonochemical hydrogen production is affected by ultrasound intensity and frequency due to their significant influence on the cavitation process. Another influential factor for hydrogen production induced by cavitation is the size of active bubbles. There exists an optimum bubble size within a range at which the hydrogen production rate is maximal. The active bubble size decreases with increasing frequency and liquid temperature and increases with increasing ultrasonic intensity. In addition, the bubble temperature and the bubble content are affected by the liquid temperature which ultimately influence the hydrogen production rate.

On the other hand, although limited research has been undertaken in ultrasound-aided electrochemical production of hydrogen, it was found that ultrasound significantly enhances the electrochemical processes for hydrogen production. The efficiency of hydrogen production was improved at a range of 5-18% at high current densities by the presence of an ultrasonic field. Ultrasound aids in 10-25% of energy savings for certain concentrations of electrolytes when coupled with a high current density. The main beneficial effects caused by ultrasound in water electrolysis are cleaning and activation of the electrode surface, increasing mass transport in the bulk solution and near the boundary layer and alternating reaction pathways caused by water sonolysis. However, the area of sonoelectrochemical hydrogen production is not explored as widely as sonochemical production. Some critical parameters such as; the influence of ultrasound frequency, ultrasound power and the effect of electrode materials are required to be investigated. In addition, the investigation for the production of hydrogen from nonaqueous solutions as well as full quantitation of produced hydrogen is necessary for the industrial application of this technology.

6. References

[1] C. Coutanceau, S. Baranton, and T. Audichon, *Hydrogen Electrochemical Production*. Cambridge: Academic Press, 2018.

[2] J. Turner *et al.*, "Renewable hydrogen production," *Int. J. Energy Res.*, vol. 32, pp. 379–407, 2008.

[3] C. M. Kalamaras and a. M. Efstathiou, "Hydrogen Production Technologies: Current State and Future Developments," *Conf. Pap. Energy*, vol. 2013, p. 9, 2013.

[4] S. Merouani and O. Hamdaoui, "The size of active bubbles for the production of hydrogen in sonochemical reaction field," *Ultrason. Sonochem.*, vol. 32, pp. 320–327, 2016.

[5] "IOR eneregy.List of common conversion factors (Engineering conversion factors)." [Online]. Available: https://web.archive.org/web/20100825042309/http://www.ior.com.au/ecflist.html. [Accessed: 21-Mar-2018].

[6] "Envestra Limited.Natural Gas Archived." [Online]. Available: https://web.archive.org/web/20081010202138/http://www.natural-gas.com.au/about/references.html. [Accessed: 21-Mar-2018].

[7] "SPECIFIC ENERGY AND ENERGY DENSITY OF FUELS." [Online]. Available: https://neutrium.net/properties/specific-energy-and-energy-density-of-fuels/. [Accessed: 21-Mar-2018].

[8] "Module 1: Hydrogen Properties," *Hydrogen Fuel Cell Engines and Related Technologies*, 2001. [Online]. Available: https://www.energy.gov/sites/prod/files/2014/03/f12/fcm01r0.pdf. [Accessed: 21-Mar-2018].

[9] S. Merouani, O. Hamdaoui, Y. Rezgui, and M. Guemini, "Mechanism of the sonochemical production of hydrogen," *Int. J. Hydrogen Energy*, vol. 40, no. 11, pp. 4056–4064, 2015.

[10] B. G. Pollet, *Power Ultrasound in Electrochemistry: From Versatile Laboratory Tool to Engineering Solution*. 2012.

[11] J. Klima, "Application of ultrasound in electrochemistry. An overview of mechanisms and design of experimental arrangement," *Ultrasonics*, vol. 51, no. 2, pp. 202–209, 2011.

[12] J. M. Ogden, M. M. Steinbugler, and T. G. Kreutz, "Comparison of hydrogen, methanol and gasoline as fuels for fuel cell vehicles: implications for vehicle design and infrastructure development," *J. Power Sources*, vol. 79, no. 2, pp. 143–168, 1999.

[13] M. Onozaki, K. Watanabe, T. Hashimoto, H. Saegusa, and Y. Katayama, "Hydrogen production by the partial oxidation and steam reforming of tar from hot coke oven gas," *Fuel*, vol. 85, no. 2, pp. 143–149, 2006.

1102 [14] H. Song, L. Zhang, R. B. Watson, D. Braden, and U. S. Ozkan, "Investigation of bio-ethanol
1103 steam reforming over cobalt-based catalysts," *Catal. Today*, vol. 129, no. 3–4, pp. 346–354, 2007.

1104 [15] B. Sørensen, *Hydrogen and Fuel Cells*. Oxford: Academic Press, 2005.

1105 [16] T. Nozaki, N. Muto, S. Kado, and K. Okazaki, "Minimum energy requirement for methane steam
1106 reforming in plasma-catalyst reactor," *Prepr. Pap.-Am. Chem. Soc., Div. ...*, vol. 49, no. c, pp.
1107 179–180, 2004.

1108 [17] M. Melaina, M. Penev, and D. Heimiller, "Resource Assessment for Hydrogen Production
1109 Hydrogen Production Potential from Fossil and Renewable Energy Resources," *Natl. Renew.*
1110 *Energy Lab. Tech. Rep.*, no. NREL/TP-5400-55626, 2013.

1111 [18] P. L. Spath and M. K. Mann, "Life Cycle Assessment of Hydrogen Production via Natural Gas
1112 Steam Reforming," *Natl. Renew. Energy Lab. DOE, U.S., Tech. Rep.*, no. NREL/MP-560-35404,
1113 2001.

1114 [19] L. Bromberg, D. R. Cohn, A. Rabinovich, C. O'Brien, and S. Hochgreb, "Plasma reforming of
1115 methane," *Energy and Fuels*, vol. 12, no. 1, pp. 11–18, 1998.

1116 [20] N. S. Arvindan, B. Rajesh, M. Madhivanan, and R. Pattabiraman, "Hydrogen generation from
1117 natural gas and methanol for use in electrochemical energy conversion systems (fuel cell)," *Indian*
1118 *J. Eng. Mater. Sci.*, vol. 6, pp. 73–86, 1999.

1119 [21] R. E. Stoll and F. von Linde, "Hydrogen-what are the costs?," *Hydrocarb. Process.*, pp. 42–46,
1120 2000.

1121 [22] S. a Sherif, D. Y. Goswami, E. K. (Lee) Stefanakos, and D. A. Steinfeld, "Handbook of Hydrogen
1122 Energy," *CRC Press*, p. 960, 2014.

1123 [23] A. Pettinau, F. Ferrara, and C. Amorino, "CO2-free hydrogen production in a coal gasification
1124 pilot plant," in *1st International Conference on Sustainable Fossil Fuels for Future Energy –*
1125 *S4FE 2009*, 2009.

1126 [24] A. Corti and L. Lombardi, "Biomass integrated gasification combined cycle with reduced
1127 CO2emissions: Performance analysis and life cycle assessment (LCA)," *Energy*, vol. 29, no. 12–
1128 15 SPEC. ISS., pp. 2109–2124, 2004.

1129 [25] K. L. Hohn and L. D. Schmidt, "Partial oxidation of methane to syngas at high space velocities
1130 over Rh-coated spheres," *Appl. Catal. A Gen.*, vol. 211, no. 1, pp. 53–68, 2001.

1131 [26] J. J. Krummenacher, K. N. West, and L. D. Schmidt, "Catalytic partial oxidation of higher
1132 hydrocarbons at millisecond contact times: Decane, hexadecane, and diesel fuel," *J. Catal.*, vol.
1133 215, no. 2, pp. 332–343, 2003.

1134 [27] A. Holmen, "Direct conversion of methane to fuels and chemicals," *Catal. Today*, vol. 142, no. 1–

2, pp. 2–8, 2009.

[28] K. Aasberg-Petersen *et al.*, "Technologies for large-scale gas conversion," *Appl. Catal. A Gen.*, vol. 221, no. 1–2, pp. 379–387, 2001.

[29] J. R. Rostrup-Nielsen, T. S. Christensen, and I. Dybkjaer, "Steam reforming of liquid hydrocarbons," *Stud. Surf. Sci. Catal.*, vol. 113, pp. 81–95, Jan. 1998.

[30] T. A. Semelsberger, L. F. Brown, R. L. Borup, and M. A. Inbody, "Equilibrium products from autothermal processes for generating hydrogen-rich fuel-cell feeds," *Int. J. Hydrogen Energy*, vol. 29, no. 10, pp. 1047–1064, 2004.

[31] F. Joensen and J. R. Rostrup-Nielsen, "Conversion of hydrocarbons and alcohols for fuel cells," *J. Power Sources*, vol. 105, no. 2, pp. 195–201, 2002.

[32] S. Ayabe *et al.*, "Catalytic Autothermal Reforming of Methane and Propane over Supported Metal Catalysts," *Appl. Catal. A Gen.*, vol. 241, no. 1, pp. 261–269, 2003.

[33] L. Bromberg, D. Cohn, and A. Rabinovich, "Plasma Reformer-Fuel Cell System For Decentralized Power Applications," *Int. J. Hydrogen Energy*, vol. 22, no. 1, pp. 83–94, 1997.

[34] L. Bromberg, "Plasma catalytic reforming of methane," *Int. J. Hydrogen Energy*, vol. 24, no. 12, pp. 1131–1137, 1999.

[35] M. F. Demirbas, "Hydrogen from various biomass species via pyrolysis and steam gasification processes," *Energy Sources, Part A Recover. Util. Environ. Eff.*, vol. 28, no. 3, pp. 245–252, 2006.

[36] M. Asadullah, S. I. Ito, K. Kunimori, M. Yamada, and K. Tomishige, "Energy efficient production of hydrogen and syngas from biomass: Development of low-temperature catalytic process for cellulose gasification," *Environ. Sci. Technol.*, vol. 36, no. 20, pp. 4476–4481, 2002.

[37] S. Karellas, "Production of Hydrogen from Renewable Resources," *SciVerse Sci.*, vol. 5, pp. 97–117, 2015.

[38] J. Zhang, "Hydrogen Production by Biomass Gasification in Supercritical Water," *Cent. Appl. Energy Res.*, vol. 19, no. 6, pp. 2–7, 2008.

[39] S. N. Reddy, S. Nanda, A. K. Dalai, and J. A. Kozinski, "Supercritical water gasification of biomass for hydrogen production," *Int. J. Hydrogen Energy*, vol. 39, no. 13, pp. 6912–6926, 2014.

[40] D. Wang, S. Czernik, D. Montané, M. Mann, and E. Chornet, "Biomass to Hydrogen via Fast Pyrolysis and Catalytic Steam Reforming of the Pyrolysis Oil or Its Fractions," *Ind. Eng. Chem. Res.*, vol. 36, no. 5, pp. 1507–1518, 1997.

[41] D. B. Levin, L. Pitt, and M. Love, "Biohydrogen production: Prospects and limitations to practical application," *Int. J. Hydrogen Energy*, vol. 29, no. 2, pp. 173–185, 2004.

[42] I. K. Kapdan and F. Kargi, “Bio-hydrogen production from waste materials,” *Enzyme Microb. Technol.*, vol. 38, no. 5, pp. 569–582, 2006.

[43] I. A. Panagiotopoulos, “Dark Fermentative Hydrogen Production from Lignocellulosic Biomass,” in *Production of Hydrogen from Renewable Resources*, Z. Fang, R. L. Smith Jr., and X. Qi, Eds. Dordrecht: Springer Netherlands, 2015, pp. 3–40.

[44] A. Konieczny, K. Mondal, T. Wiltowski, and P. Dydo, “Catalyst development for thermocatalytic decomposition of methane to hydrogen,” *Int. J. Hydrogen Energy*, vol. 33, no. 1, pp. 264–272, 2008.

[45] A. L. Dicks, “FUEL CELLS – MOLTEN CARBONATE FUEL CELLS | Cathodes,” in *Encyclopedia of Electrochemical Power Sources*, Elsevier, 2009, pp. 462–466.

[46] J. Ivy, “Summary of Electrolytic Hydrogen Production Milestone Completion Report,” *Natl. Renew. Energy Lab.*, 2004.

[47] K. Chen, D. Dong, and S. P. Jiang, “Hydrogen Production from Water and Air Through Solid Oxide Electrolysis,” in *Production of Hydrogen from Renewable Resources*, Z. Fang, R. L. Smith Jr., and X. Qi, Eds. Dordrecht: Springer Netherlands, 2015, pp. 223–248.

[48] M. Carmo, D. L. Fritz, J. Mergel, and D. Stolten, “A comprehensive review on PEM water electrolysis,” *Int. J. Hydrogen Energy*, vol. 38, no. 12, pp. 4901–4934, 2013.

[49] M. Wang, Z. Wang, X. Gong, and Z. Guo, “The intensification technologies to water electrolysis for hydrogen production - A review,” *Renew. Sustain. Energy Rev.*, vol. 29, pp. 573–588, 2014.

[50] A. Ursua, L. M. Gandia, and P. Sanchis, “Hydrogen Production From Water Electrolysis: Current Status and Future Trends,” *Proc. IEEE*, vol. 100, no. 2, pp. 410–426, 2012.

[51] A. Hauch, S. D. Ebbesen, S. H. Jensen, and M. Mogensen, “Highly efficient high temperature electrolysis,” *J. Mater. Chem.*, vol. 18, no. 20, pp. 2331–2340, 2008.

[52] L. Hu, “Molten carbonate fuel cells for electrolysis,” KTH Royal Institute of Technology, 2016.

[53] R. Hino and X. L. Yan, “Hydrogen Production from Nuclear Energy,” in *Hydrogen Fuel: Production, Transport, and Storage*, R. B. Gupta, Ed. Boca Raton: CRC Press, 2008, pp. 127–159.

[54] C. N. Hamelinck and A. P. C. Faaij, “Future prospects for production of methanol and hydrogen from biomass,” *J. Power Sources*, vol. 111, no. 1, pp. 1–22, 2002.

[55] S.-E. Lindquist and C. Fell, “FUELS – HYDROGEN PRODUCTION | Photoelectrolysis,” in *Encyclopedia of Electrochemical Power Sources*, Elsevier, 2009, pp. 369–383.

[56] M. Legay, N. Gondrexon, S. Le Person, P. Boldo, and A. Bontemps, “Enhancement of heat transfer by ultrasound: Review and recent advances,” *Int. J. Chem. Eng.*, vol. 2011, 2011.

[57] K. Yasui, *Acoustic Cavitation and Bubble Dynamics*. SpringerBriefs in Molecular Science: Ultrasound and Sonochemistry, 2018.

[58] T. Leong, M. Ashokkumar, and S. Kentish, "The fundamentals of power ultrasound—a review," *Acoust. Aust*, vol. 39, no. 2, pp. 54–63, 2011.

[59] K. S. Suslick, "Sonochemistry," *Science (80-.).*, vol. 247, pp. 1439–1445, 1990.

[60] T. J. Mason, *Sonochemistry : The Uses of Ultrasound in Chemistry*. Cambridge: Royal Society of Chemistry, 1990.

[61] K. Yasui, "Unsolved Problems in Acoustic Cavitation," in *Handbook of Ultrasonics and Sonochemistry*, 2016, pp. 259–292.

[62] D. R. Lide and H. P. R. Frederikse, *Handbook of chemistry and physics.*, 75th ed. Florida: Boca Raton: CRC Press, 1994.

[63] A. Henglein, *Contributions to various aspects of cavitation chemistry*, vol. 3. London: JAI Press, 1993.

[64] S. Merouani, O. Hamdaoui, Y. Rezgui, and M. Guemini, "Sensitivity of free radicals production in acoustically driven bubble to the ultrasonic frequency and nature of dissolved gases," *Ultrason. Sonochem.*, vol. 22, no. JULY 2014, pp. 41–50, 2015.

[65] M. Ashokkumar and F. Grieser, "ULTRASOUND ASSISTED CHEMICAL PROCESSES," *Reviews in Chemical Engineering*, vol. 15. p. 41, 1999.

[66] K. S. Suslick and E. B. Flint, "Sonoluminescence from non-aqueous liquids," *Nature*, vol. 330, p. 553, Dec. 1987.

[67] N. MORIGUCHI, "The Influence of Supersonic Waves on Chemical Phenomena. III The Influence on the Concentration Polarisation," *Nippon KAGAKU KAISHI*, vol. 55, no. 8, pp. 749–750, 1934.

[68] V. Frenkel, R. Gurka, A. Liberzon, U. Shavit, and E. Kimmel, "Preliminary investigations of ultrasound induced acoustic streaming using particle image velocimetry," *Ultrasonics*, vol. 39, no. 3, p. 153—156, Apr. 2001.

[69] A. Kumar, T. Kumaresan, A. B. Pandit, and J. B. Joshi, "Characterization of flow phenomena induced by ultrasonic horn," *Chem. Eng. Sci.*, vol. 61, no. 22, pp. 7410–7420, Nov. 2006.

[70] S. A. Elder, "Cavitation microstreaming," *J. Acoust. Soc. Am.*, vol. 31, no. 54, 1959.

[71] J. or minute] Gonzalez-Garcia, J. Iniesta, A. Aldaz, and V. Montiel, "Effects of ultrasound on the electrodeposition of lead dioxide on glassy carbon electrodes," *New J. Chem.*, vol. 22, no. 4, pp. 343–349, 1998.

[72] S. H. Zadeh, "Hydrogen Production via Ultrasound-Aided Alkaline Water Electrolysis," *J. Autom. Control Eng.*, vol. 2, no. 1, pp. 103–109, 2014.

[73] K. Makino, M. Mossoba, and P. Riesz, "Chemical effects of ultrasound on aqueous solutions. Formation of Evidence for OH an H by spein trapping," *J. Am. Chem. SOC*, vol. 104, no. 21, pp. 3537–3539, 1982.

[74] X. Fang, G. Mark, and C. von Sonntag, "OH radical formation by ultrasound in aqueous solutions Part I: the chemistry underlying the terephthalate dosimeter," *Ultrason. Sonochem.*, vol. 3, no. 1, pp. 57–63, Feb. 1996.

[75] M. Ashokkumar, T. Niblett, L. Tantiongco, and F. Grieser, "Sonochemical Degradation of Sodium Dodecylbenzene Sulfonate in Aqueous Solutions," *Aust. J. Chem.*, vol. 56, no. 10, pp. 1045–1049, Sep. 2003.

[76] S. Koda, T. Kimura, T. Kondo, and H. Mitome, "A standard method to calibrate sonochemical efficiency of an individual reaction system," *Ultrason. Sonochem.*, vol. 10, no. 3, p. 149—156, May 2003.

[77] D. Comeskey, O. A. Larparadsudthi, T. J. Mason, and L. Paniwnyk, "The use of a range of ultrasound frequencies to reduce colouration caused by dyes," *Water Sci. Technol.*, vol. 66, no. 10, pp. 2251–2257, 2012.

[78] E. J. Hart and A. Henglein, "Free radical and free atom reactions in the sonolysis of aqueous iodide and formate solutions," *J. Phys. Chem.*, vol. 89, no. 20, pp. 4342–4347, 1985.

[79] L. Villeneuve, L. Alberti, J. P. Steghens, J. M. Lancelin, and J. L. Mestas, "Assay of hydroxyl radicals generated by focused ultrasound," *Ultrason. Sonochem.*, vol. 16, no. 3, pp. 339–344, 2009.

[80] T. J. Mason, J. P. Lorimer, D. M. Bates, and Y. Zhao, "Dosimetry in sonochemistry: the use of aqueous terephthalate ion as a fluorescence monitor," *Ultrason. - Sonochemistry*, vol. 1, no. 2, 1994.

[81] Y. Iida, K. Yasui, T. Tuziuti, and M. Sivakumar, "Sonochemistry and its dosimetry," *Microchem. J.*, vol. 80, no. 2, pp. 159–164, 2005.

[82] L. Milne, I. Stewart, and D. H. Bremner, "Comparison of hydroxyl radical formation in aqueous solutions at different ultrasound frequencies and powers using the salicylic acid dosimeter," *Ultrason. Sonochem.*, vol. 20, no. 3, pp. 984–989, May 2013.

[83] A. G. Chakinala, P. R. Gogate, A. E. Burgess, and D. H. Bremner, "Intensification of hydroxyl radical production in sonochemical reactors," *Ultrason. Sonochem.*, vol. 14, no. 5, pp. 509–514, 2007.

[84] K. Hirano and T. Kobayashi, "Coumarin fluorometry to quantitatively detectable OH radicals in ultrasound aqueous medium," *Ultrason. Sonochem.*, vol. 30, pp. 18–27, 2016.

1266 [85] H. Zhang, L. Duan, and D. Zhang, “Decolorization of methyl orange by ozonation in combination
1267 with ultrasonic irradiation,” *J. Hazard. Mater.*, vol. 138, no. 1, pp. 53–59, 2006.

1268 [86] L. Wang, L. Zhu, W. Luo, Y. Wu, and H. Tang, “Drastically enhanced ultrasonic decolorization of
1269 methyl orange by adding CCl4,” *Ultrason. Sonochem.*, vol. 14, no. 2, pp. 253–258, 2007.

1270 [87] W. Luo, M. E. Abbas, L. Zhu, K. Deng, and H. Tang, “Rapid quantitative determination of
1271 hydrogen peroxide by oxidation decolorization of methyl orange using a Fenton reaction system,”
1272 *Anal. Chim. Acta*, vol. 629, no. 1–2, pp. 1–5, 2008.

1273 [88] M. Cai *et al.*, “Sono-advanced Fenton decolorization of azo dye Orange G: Analysis of synergistic
1274 effect and mechanisms,” *Ultrason. Sonochem.*, vol. 31, pp. 193–200, 2016.

1275 [89] B. Yim, H. Okuno, Y. Nagata, R. Nishimura, and Y. Maeda, “Sonolysis of surfactants in aqueous
1276 solutions: An accumulation of solute in the interfacial region of the cavitation bubbles,” *Ultrason.*
1277 *Sonochem.*, vol. 9, no. 4, pp. 209–213, 2002.

1278 [90] E. Dalodière, M. Virot, P. Moisy, and S. I. Nikitenko, “Effect of ultrasonic frequency on
1279 H2O2sonochemical formation rate in aqueous nitric acid solutions in the presence of oxygen,”
1280 *Ultrason. Sonochem.*, vol. 29, no. 2, pp. 198–204, 2016.

1281 [91] V. Morosini, T. Chave, M. Virot, P. Moisy, and S. I. Nikitenko, “Sonochemical water splitting in
1282 the presence of powdered metal oxides,” *Ultrason. Sonochem.*, vol. 29, pp. 512–516, 2016.

1283 [92] Y. Yang, W.-Z. Gai, Z.-Y. Deng, and J.-G. Zhou, “Hydrogen generation by the reaction of Al with
1284 water promoted by an ultrasonically prepared Al(OH)3 suspension,” *Int. J. Hydrogen Energy*, vol.
1285 39, no. 33, pp. 18734–18742, Nov. 2014.

1286 [93] H. Harada, “Isolation of hydrogen from water and/or artificial seawater by sonophotocatalysis
1287 using alternating irradiation method,” *Int. J. Hydrogen Energy*, vol. 26, no. 4, pp. 303–307, Apr.
1288 2001.

1289 [94] E. Elbeshbishy, H. Hafez, and G. Nakhla, “Hydrogen production using sono-biohydrogenator,”
1290 *Int. J. Hydrogen Energy*, vol. 36, no. 2, pp. 1456–1465, Jan. 2011.

1291 [95] A. Gadhe, S. S. Sonawane, and M. N. Varma, “Evaluation of ultrasonication as a treatment
1292 strategy for enhancement of biohydrogen production from complex distillery wastewater and
1293 process optimization,” *Int. J. Hydrogen Energy*, vol. 39, no. 19, pp. 10041–10050, Jun. 2014.

1294 [96] K. S. Suslick and D. J. Flannigan, “Inside a Collapsing Bubble: Sonoluminescence and the
1295 Conditions During Cavitation,” *Annu. Rev. Phys. Chem.*, vol. 59, no. 1, pp. 659–683, 2008.

1296 [97] E. J. Hart and A. Henglein, “Sonochemistry of aqueous solutions: H2-O2 combustion in cavitation
1297 bubbles,” *J. Phys. Chem.*, vol. 91, no. 11, pp. 3654–3656, 1987.

1298 [98] Y. G. Adewuyi, “Sonochemistry: Environmental Science and Engineering Applications,” *Ind.*

Eng. Chem. Res., vol. 40, no. 22, pp. 4681–4715, 2001.

[99] C. H. Fischer, E. J. Hart, and A. Henglein, "Hydrogen/deuterium isotope exchange in the molecular deuterium-water system under the influence of ultrasound," *J. Phys. Chem.*, vol. 90, no. 2, pp. 222–224, 1986.

[100] E. J. Hart, C. H. Fischer, and A. Henglein, "Isotopic exchange in the sonolysis of aqueous solutions containing nitrogen-14 and nitrogen-15 molecules," *J. Phys. Chem.*, vol. 90, no. 22, pp. 5989–5991, 1986.

[101] P. L. Gentili, M. Penconi, F. Ortica, F. Cotana, F. Rossi, and F. Elisei, "Synergistic effects in hydrogen production through water sonophotolysis catalyzed by new La2xGa2yIn2(1−x−y)O3 solid solutions," *Int. J. Hydrogen Energy*, vol. 34, no. 22, pp. 9042–9049, Nov. 2009.

[102] M. Anbar and I. Pecht, "The Sonolytic Decomposition of Organic Solutes in Dilute Aqueous Solutions. I. Hydrogen Abstraction from Sodium Formate," *J. Phys. Chem.*, vol. 68, no. 6, pp. 1460–1462, 1964.

[103] M. Anbar and I. Pecht, "On the Sonochemical Formation of Hydrogen Peroxide in Water," *J. Phys. Chem.*, vol. 68, no. 2, pp. 352–355, 1964.

[104] C. H. Fischer, E. J. Hart, and A. Henglein, "Ultrasonic irradiation of water in the presence of oxygen 18,18O2: isotope exchange and isotopic distribution of hydrogen peroxide," *J. Phys. Chem.*, vol. 90, no. 9, pp. 1954–1956, 1986.

[105] M. Gutierrez, A. Henglein, and J. K. Dohrmann, "Hydrogen atom reactions in the sonolysis of aqueous solutions," *J. Phys. Chem.*, vol. 91, no. 27, pp. 6687–6690, 1987.

[106] S. Merouani, O. Hamdaoui, Y. Rezgui, and M. Guemini, "Computational engineering study of hydrogen production via ultrasonic cavitation in water," *Int. J. Hydrogen Energy*, vol. 41, no. 2, pp. 832–844, 2016.

[107] A. Henglein, "Sonolysis of carbon dioxide, nitrous oxide and methane in aqueous solution," *Z.Naturforsch.*, vol. 40 b, pp. 100–107, 1985.

[108] Y. Wang *et al.*, "Sonochemical hydrogen production efficiently catalyzed by Au/TiO2," *J. Phys. Chem. C*, vol. 114, no. 41, pp. 17728–17733, 2010.

[109] P. Kanthale, M. Ashokkumar, and F. Grieser, "Sonoluminescence, sonochemistry (H2O2 yield) and bubble dynamics: Frequency and power effects," *Ultrason. Sonochem.*, vol. 15, no. 2, pp. 143–150, Feb. 2008.

[110] S. Merouani, H. Ferkous, O. Hamdaoui, Y. Rezgui, and M. Guemini, "A method for predicting the number of active bubbles in sonochemical reactors," *Ultrason. Sonochem.*, vol. 22, no. SEPTEMBER, pp. 51–58, 2015.

[111] C. H. Fischer, E. J. Hart, and A. Henglein, “H/D isotope exchange in the D2-H2O system under the influence of ultrasound,” *J. Phys. Chem.*, vol. 17, no. 20, pp. 222–224, 198AD.

[112] J. Buettner, M. Gutierrez, and A. Henglein, “Sonolysis of water-methanol mixtures,” *J. Phys. Chem.*, vol. 95, no. 4, pp. 1528–1530, 1991.

[113] L. Venault, “De l’influence des ultrasons sur la reactivite de l’uranium (u(iv)/u(vi)) et du plutonium (pu(iii)/pu(iv)) en solution aqueuse nitrique,” Universite de Paris XI Orsay, 1997.

[114] D. Sunartio, M. Ashokkumar, and F. Grieser, “Study of the Coalescence of Acoustic Bubbles as a Function of Frequency, Power, and Water-Soluble Additives,” *J. Am. Chem. Soc.*, vol. 129, no. 18, pp. 6031–6036, 2007.

[115] S. Merouani, H. Ferkous, O. Hamdaoui, Y. Rezgui, and M. Guemini, “New interpretation of the effects of argon-saturating gas toward sonochemical reactions,” *Ultrason. Sonochem.*, vol. 23, no. SEPTEMBER, pp. 37–45, 2015.

[116] I. Hua and M. R. Hoffmann, “Optimization of Ultrasonic Irradiation as an Advanced Oxidation Technology,” *Environ. Sci. Technol.*, vol. 31, no. 8, pp. 2237–2243, 1997.

[117] F. Guzman-Duque, C. Pétrier, C. Pulgarin, G. Peñuela, and R. A. Torres-Palma, “Effects of sonochemical parameters and inorganic ions during the sonochemical degradation of crystal violet in water,” *Ultrason. Sonochem.*, vol. 18, no. 1, pp. 440–446, Jan. 2011.

[118] D. G. Wayment and D. J. Casadonte, “Frequency effect on the sonochemical remediation of alachlor,” *Ultrason. Sonochem.*, vol. 9, no. 5, pp. 251–257, Oct. 2002.

[119] R. A. Torres, C. Pétrier, E. Combet, M. Carrier, and C. Pulgarin, “Ultrasonic cavitation applied to the treatment of bisphenol A. Effect of sonochemical parameters and analysis of BPA by-products,” *Ultrason. Sonochem.*, vol. 15, no. 4, pp. 605–611, Apr. 2008.

[120] M. A. Beckett and I. Hua, “Impact of Ultrasonic Frequency on Aqueous Sonoluminescence and Sonochemistry,” *J. Phys. Chem. A*, vol. 105, no. 15, pp. 3796–3802, 2001.

[121] E. L. Mead, R. G. Sutherland, and R. E. Verrall, “The effect of ultrasound on water in the presence of dissolved gases,” *Can. J. Chem.*, vol. 54, no. 7, pp. 1114–1120, 1976.

[122] K. Okitsu, T. Suzuki, N. Takenaka, H. Bandow, R. Nishimura, and Y. Maeda, “Acoustic Multibubble Cavitation in Water: A New Aspect of the Effect of a Rare Gas Atmosphere on Bubble Temperature and Its Relevance to Sonochemistry,” *J. Phys. Chem. B*, vol. 110, no. 41, pp. 20081–20084, 2006.

[123] M. Marguli and Y. Didenko, “Energetics and mechanism of acoustochemical reactions. Yields of hydrogen and hydrogen peroxide in different aqueous systems,” *Russ J Phys Chem*, vol. 58, no. 6, pp. 848–850, 1985.

[124] C. Gong and D. P. Hart, "Ultrasound induced cavitation and sonochemical yields," *J. Acoust. Soc. Am.*, vol. 104, no. 5, pp. 2675–2682, 1998.

[125] S. De Li, C. C. Wang, and C. Y. Chen, "Water electrolysis in the presence of an ultrasonic field," *Electrochim. Acta*, vol. 54, no. 15, pp. 3877–3883, 2009.

[126] H. Cheng, K. Scott, and C. Ramshaw, "Intensification of Water Electrolysis in a Centrifugal Field," *J. Electrochem. Soc.*, vol. 149, no. 11, p. D172, 2002.

[127] C. Budischak, C. Honsberg, and R. L. Opila, "Electroanalytic effects of ultrasound on a hydrogen evolution reaction in KOH," *Conf. Rec. IEEE Photovolt. Spec. Conf.*, 2008.

[128] D. J. Walton, L. D. Burket, and M. M. Murphy, "Sonoelectrochemistry : and Oxygen Evolution Chlorine , Hydrogen At Platinised Platinum," *Electrochim. Acta*, vol. 41, no. 17, pp. 2747–2751, 1996.

[129] H. K. Abdel-Aal, K. M. Zohdy, and M. A. Kareem, "Hydrogen Production Using Sea Water Electrolysis," *Open Fuel Cells J.*, vol. 3, pp. 1–7, 2010.

[130] F. Cataldo, "Effects of ultrasound on the yield of hydrogen and chlorine during electrolysis of aqueous solutions of NaCl or HCl," *J. Electroanal. Chem.*, vol. 332, no. 1–2, pp. 325–331, 1992.

[131] H. Matsushima, Y. Fukunaka, and K. Kuribayashi, "Water electrolysis under microgravity: Part II. Description of gas bubble evolution phenomena," *Electrochim. Acta*, vol. 51, no. 20, pp. 4190–4198, May 2006.

[132] J. Li, J. Xue, Z. Tan, Y. Zheng, L. Zhang, and T. Beijing, "ULTRASOUND-ASSISTED ELECTROLYSIS IN NaOH SOLUTION FOR," in *EPD Congress*, 2011, pp. 919–926.

[133] K. Qian, Z. D. Chen, and J. J. J. Chen, "Bubble coverage and bubble resistance using cells with horizontal electrode," *J. Appl. Electrochem.*, vol. 28, no. 10, pp. 1141–1145, Oct. 1998.

[134] M.-Y. Lin and L.-W. Hourng, "Ultrasonic wave field effects on hydrogen production by water electrolysis," *J. Chinese Inst. Eng.*, vol. 37, no. 8, pp. 1080–1089, 2014.

[135] H. N. McMurray, "Hydrogen evolution and oxygen reduction at a titanium sonotrode," *Chem. Commun.*, no. 8, pp. 887–888, 1998.